

³¹
GArcia
69.723

⁵⁹
PRogram
140.91

¹⁶
Summer 2013
32.065



"The program has no set time limits. Research is a lifelong learning experience, and we hope to remain a resource to our students long after 'graduation'."



**Jonathan
Sokolov**

The Garcia Center for Polymers at Engineered Interfaces is a collaboration of eleven academic, industrial, and government laboratories. The Center was founded in 1996 and is named after the late Queens College professor, Narciso Garcia, a pioneer in the integration of education and research. The Garcia Center is funded by the **National Science Foundation as part of its Materials Research Science and Engineering Center (MRSEC)** program. The goal of the MRSEC is to combine the instrumentation and expertise of the participating institutions into a coordinated research program on polymer interface science. The principal focus areas include thin films, coatings, nano composites, self assembled structures, biomaterials, a and tissue engineering.

These areas address both the fundamental and applied aspects that are relevant to the development of cutting-edge technologies in both engineering and medicine. In the community, the mission of the center is to serve as a valuable resource, providing easy access for technological assistance to educational and industrial institutions. For information on the numerous programs that are available, please see our web site at:

<http://polymer.matscieng.sunysb.edu>

The Research Scholar Program offers the opportunity for high school teachers and students to perform research on the forefronts of polymer science and technology together with the Garcia faculty and staff. Students work as part of focused research teams and are taught to make original contributions of interest to the scientific community. In addition to entering national competitions, the students are encouraged to publish in revered scientific journals and present their results at national conferences.

Our goal is to convey to the students the excitement we enjoy daily in research. The program has no set time limits. Research is a lifelong learning experience, and we hope to remain a resource to our students long after "graduation".



**Miriam
Rafailovich**

**Miriam Rafailovich
Professor, Garcia MRSEC**

**Jonathan Sokolov
Professor, Garcia MRSEC**

Faculty and Staff



Dr. Chung-Chueh
(Simon) Chang,



Dr. Ying Liu



Rebecca
Isseroff
(RET)



Thomas
Van Bell
(RET)



Dr. Marcia Simon



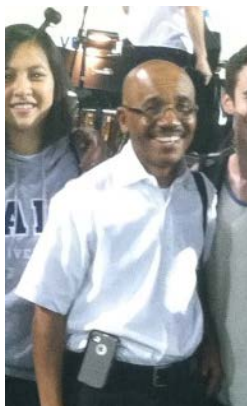
Herb Weiss (RET)



Dennis
Galanakis,
MD



Dr. Christine
Falabella



Dr. John
Luckner Jerom



Dr. Stephen
Walker



Dr. H Z Wang



Dr. Peter Brink



Maurizio Del
Poeta, MD

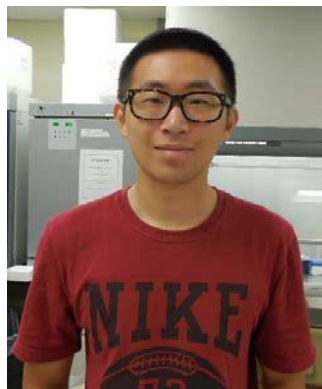


Dr. Dilip
Gersappe

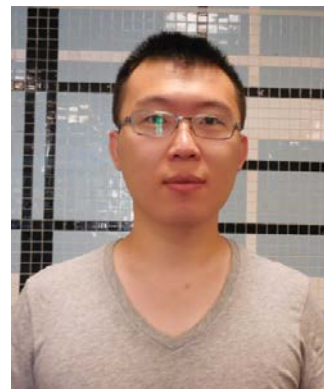
Graduate Student Researchers



Cheng Pan



Fan Yang



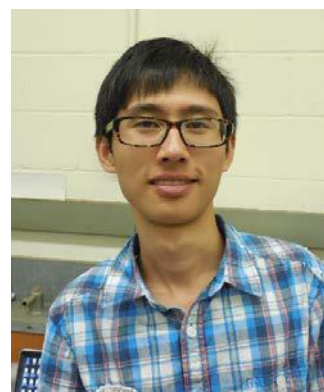
Hongfei Li



Jane Zhang



Kai Yang



Ke Zhu



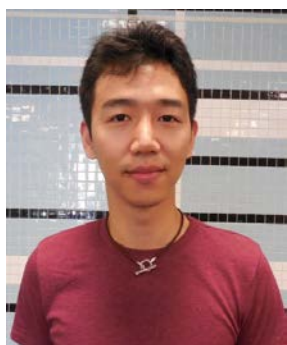
Kuan-Che Feng



Linxi Zhang



Luidi Zhang



Shan He



Sisi Qin



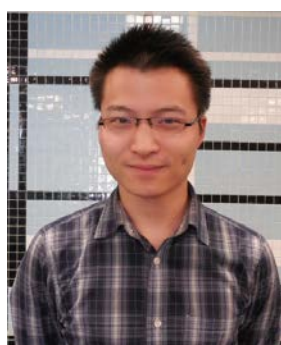
Yan Xu



Yichen Guo



Yingjie Yu



Zhenhua Yang



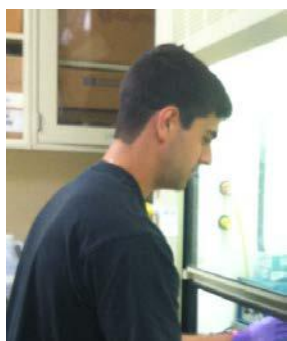
Di Xu



Zihao Chen



Ning Sun



Joseph Miccio

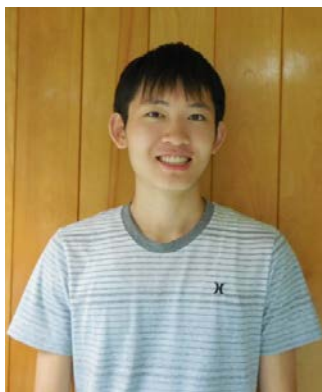


Vianney Delplace

Research Experience for Undergrads (REU)



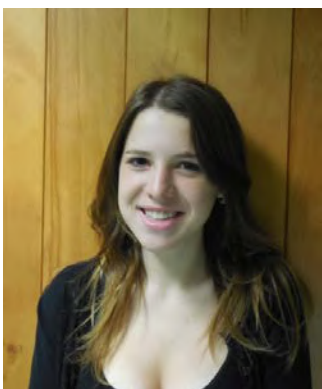
Aatman Makadia



Alexander Lee



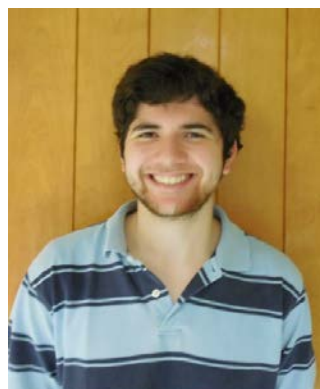
Applebaum



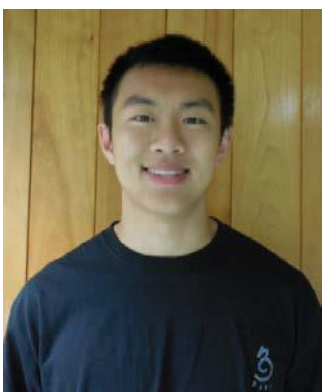
Applebaum



Andrew Chen



Benjamin Goldman



Jason Kuan



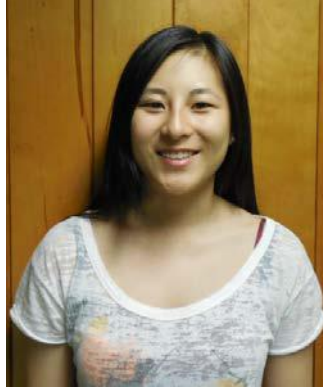
Julia Budassi



Julia Landsberg



Monika Batra



Rachel Yang



Satya Makadia



Steven Krim



Suditi Sood



Timothy Hart



Weida Zhang

Garcia Students



Aaron Argyres



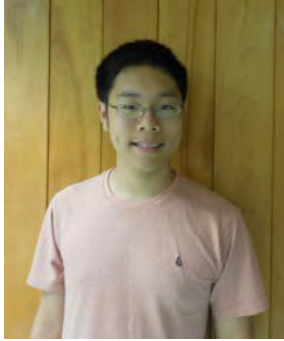
Aaron Gochman



Abraham Gross



Alec Silverstein



Alex Tang



Allison Chowdhury



Allison Lee



Amanda Shi



Benjamin Khakshoor



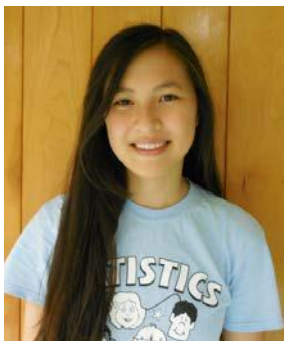
Brandon Prashad



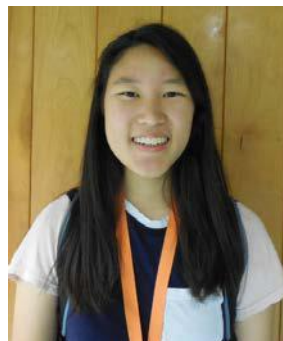
Brian Zhong



Cameron Akker



Chantel Yang



Christina Chen



Courtney Schwartz



Daniel Rudin



Daphne Chen



David Levi



Emma Zawacki



Evelyn Kandov



Forrest Butensky



Greta Huang



Hillel Lerner



Ivy Ren



Jacob Eiferman



Jacob Plaut



Jason Zarate



Jing Xian Wang



Joseph Cappadona



Joseph Jacob



Joshua Wende



Justin Silverman



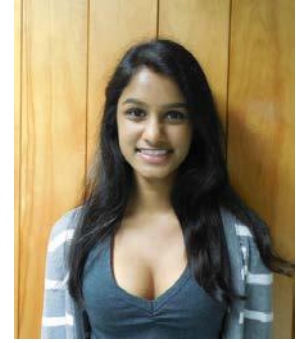
Kaveh Issapour



Kevin Liu



Kimia Ziadkhanpour



Krishana Raghubeer



Leandra Meraglia-Garcia



Leeson Chen



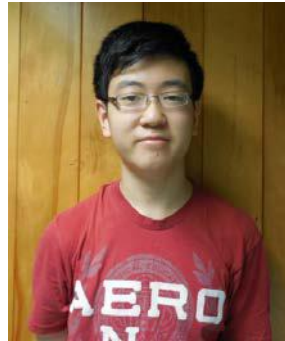
Luke Chen



Matthew Kempster



Michal Leibowitz



Min Seong Kim



Mingu Kim



Miriam Friedman



Nicolette Almer



Noah Davis



Paige Botie



Rohit Mehandru



Rose Bender



Ruiyi Gao



Ruth Kopyto



Sharon Shu



Shoshana Guterman



Siavash Parkhideh



Tuan Ahn Lam



Tyler Dougan



Tzadok Hartman



Varun Mohan



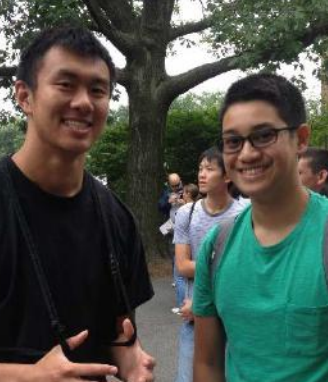
Vivek Subramaniam

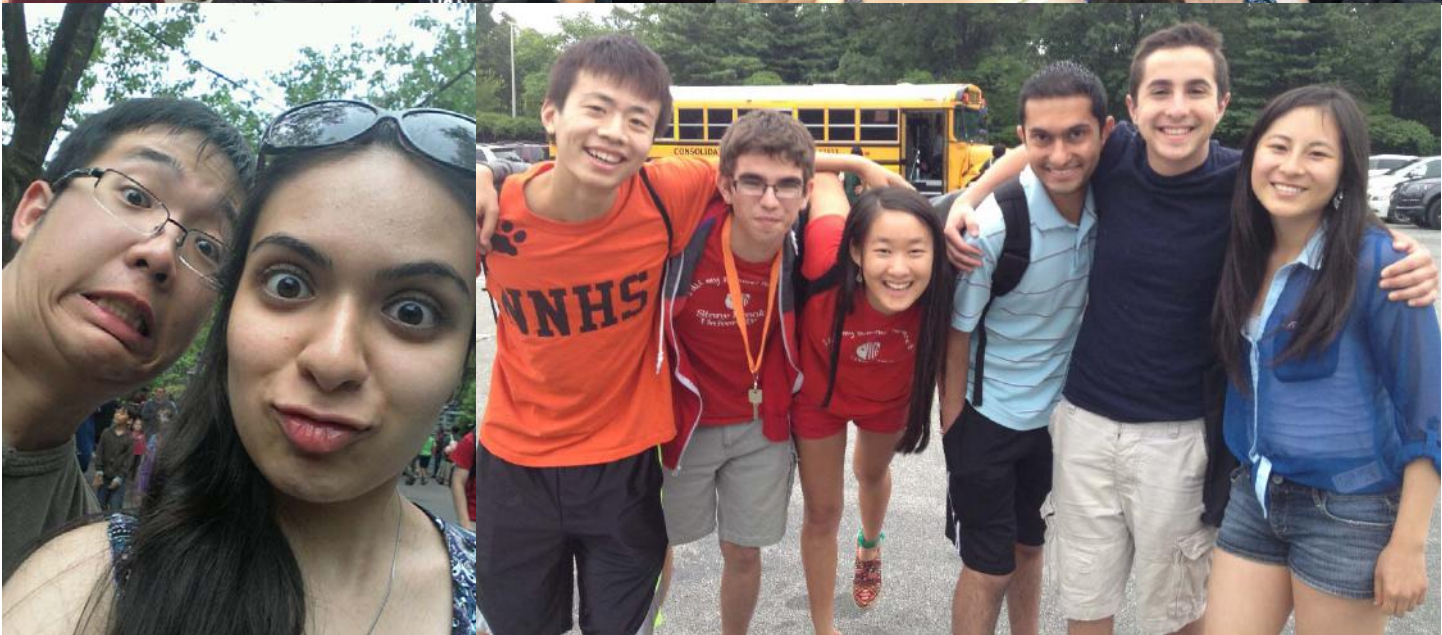


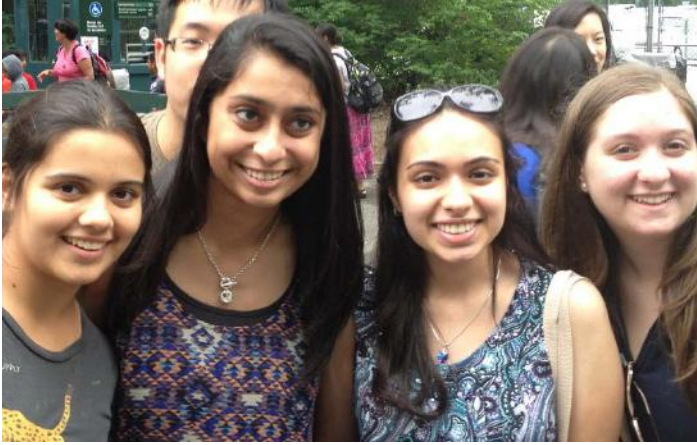
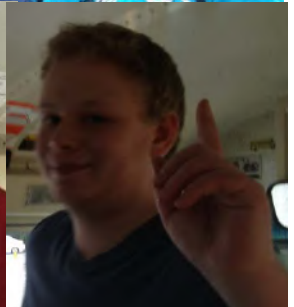
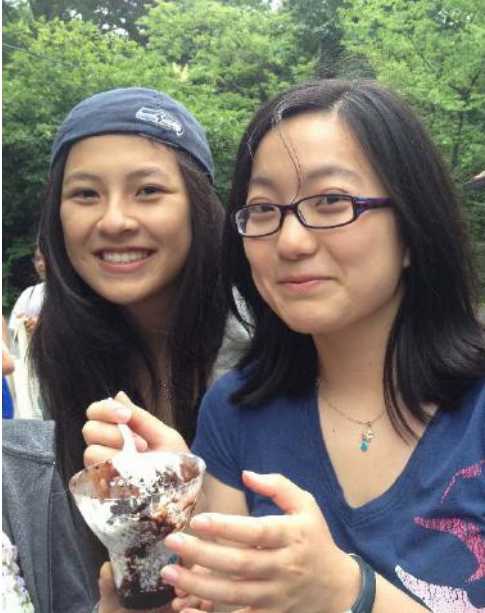
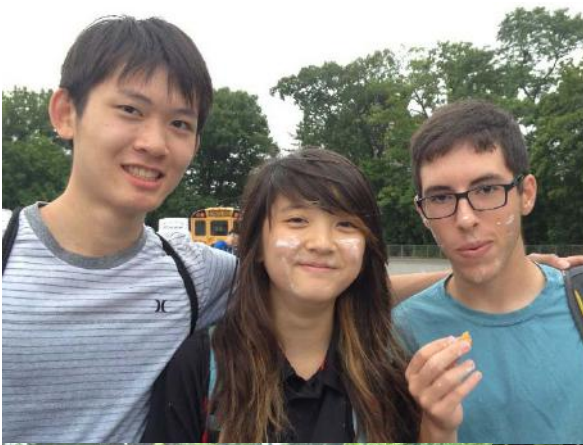
Yongyi Zhao

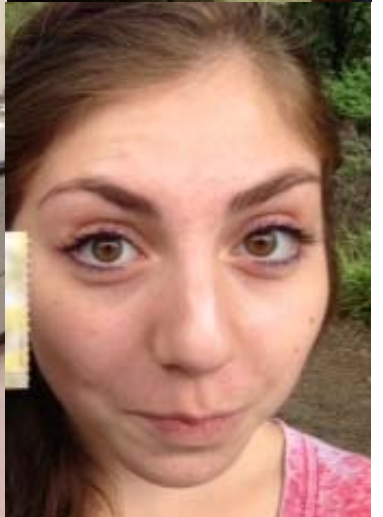
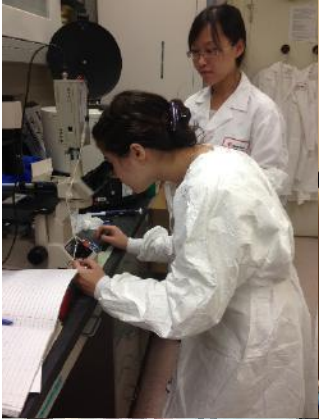
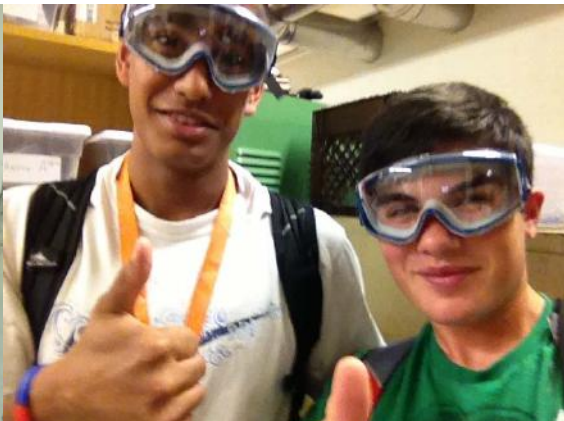


ZOO ENTRANCE

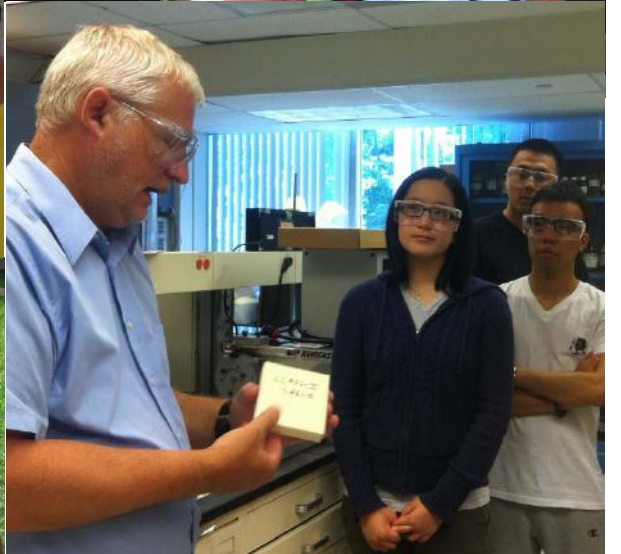
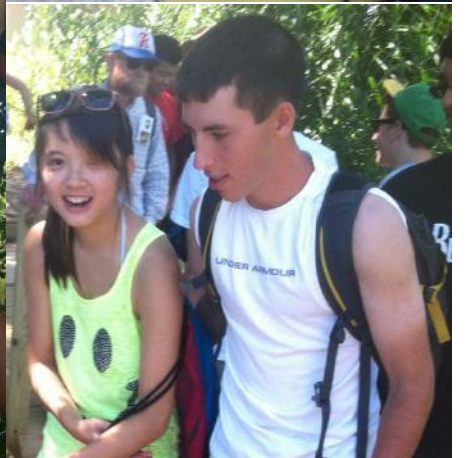












GArcia
PRogram
Summer 2013

10:00 **Musical Arrangement** : Garcia Students,
directed by Prof. John Luckner Jerome

10:10 **Opening Remarks** Senator Kenneth LaValle

10:00 **Guest Speaker: Dr. Brooke Ellison**

10:20 – 10:40 **Materials for Energy Generation**

**Chairs: Andrew Chen, Rice University; Weida Zhang, Stony Brook University;
Benjamin Goldman, Queens College**

Investigating the ability of a photovoltaic system with battery backup to power life support in case of emergency

Alex Tang, Interlake High School, Bellevue, WA

Graphene oxide coated Nafion membrane for enhanced performance in polymer electrolyte membrane fuel cells

Cameron Akker, Redmond High School, Redmond, WA

Improving Organic Polymer Solar Cell Efficiency via Active Layer Organization and the Incorporation of Graphene, Graphene Oxide, and Carbon Nanotubes

Kaveh Issapour, Syosset High School, Syosset, NY

Krishana Raghubeer, Lawrence High School, Cedarhurst, NY

Noah Davis, Earl L. Vandermeulen High School, Port Jefferson, NY

Effect of Nanoparticle Monolayer Coating of Nafion® Membrane on PEMFC Performance and Tolerance to Fuel Impurities

Rose Bender and Joshua Wende, Half Hollow Hills High School West, Dix Hills, NY

Optimization of Bulk Heterojunction Solar Cells via Phase-Separated Polymer Blends

Sharon Shu, Campbell High School, Smyrna, Georgia

Brian Zhong, Dougherty Valley High School, San Ramon, CA

Gold platinum and copper platinum nanoparticles-coated Nafion membrane for enhanced performance in polymer electrolyte membrane fuel cells

Tuan Anh Lam, Loomis Chaffee School, Windsor, CT

Au/Pt nanoparticles for increasing CO₂ tolerance in PEMFCs

Tyler Dougan, The Blake School, Minneapolis, MN

10:45 – 11:00 **Nanocomposites and Alloys**

Chairs: Steven Krim, Stony Brook University; Julia Landsberg, Queens College; Julia Budassi, Stony Brook University

Mechanical and Flame Retardant Properties of Styrene Copolymer Nanocomposites Using Different Clays

Brandon Prashad and Justin Silverman, South Side HS, Rockville Centre, NY

Erosion Testing of Plasma Sprayed Yttria-Stabilized Zirconia Coated Aluminum Substrates

Forrest Butensky, South Side High School, Rockville Centre, NY

Synergistic Effects of Graphene, Carbon Nanotube, and Copper Additives on the Thermal, Mechanical, and Flame Retardant Properties of Polypropylene

Joseph Cappadona, Lynbrook Senior High School, Lynbrook, New York

Ivy Ren, Thomas Jefferson High School for Science and Technology, Alexandria, Virginia

A multi-scale simulation: examining thermal conductivity of polymers enhanced by nanofillers of different geometries

Joseph Jacob, The Wheatley School, Old Westbury, NY

The Study of the Effects of Morphology and Porosity on Charge Capacity and Charge Rate of Graphite Anode Systems Using the Lattice Boltzmann Method

Varun Mohan, The Harker School, San Jose, CA

Nanocrystalline tungsten alloys for self-sharpening kinetic energy penetrators

Miriam Friedman, HAFTR High School, NY

11:00 – 11:15 **Novel 2D and 3D Printing Technologies;
Unusual Applications of Electrospinning Techniques**

Chairs: Monika Batra, Stony Brook University; Rachel Yang, Cornell University; Aatman Makadia; Timothy Hart, Stony Brook University

Using Three Dimensional Printing to create a Drug Eluting Scaffold
David Levi and Hillel Lerner, Rambam Mesivta High School, Lawrence NY

Novel Cimex Lectularius Trapping Mechanism Using Electrospinning Technology
Michal Leibowitz, Yeshiva University High School Girls, NY
Jacob Plaut, Rambam Mesivta High School for Boys, NY
Daniel Rudin, Half Hollow Hills High School West, Dix Hills, NY

Micro-Scale Engineering a Novel Tattoo Ink Removable by Ultrasound
Rohit Mehandru, Roslyn High School, Roslyn Heights, NY

Inkjet Printing of Human Dermal Fibroblasts and RK13 Cells for Applications in Tissue Engineering
Leeson Chen, Palm Harbor University High School, Palm Harbor, FL

Synthesis of Larger Graphene sheets from Graphene Oxide using Ink-jet Printing
Tzadok Hartman, Rambam Mesivta High School, Lawrence, NY

11:15 – 11:40 **Dermal Cells/Aging/Cancer/Adipocytes/Cell Migration/Fibrinogen**

Chairs: Ariella Applebaum, Stern College for Women; Elianna Applebaum, Stern College for Women; Jason Kuan, Amherst College

Influence of Hydrogel Substrate on Pseudorabies Virus Infection
Courtney Schwartz, The Wheatley School, Old Westbury, NY
Chantel Yang, Commack High School, Commack, NY

The Effect of Dermal Fibroblast Age on cell Migration Rates on Electrospun Scaffolds for Wound Healing
Christina Chen, Diamond Bar High School, Diamond Bar, CA
Kevin Liu, Interlake High School, Bellevue, WA

Analysis of the migration and traction forces of dermal fibroblasts on hydrogel surfaces of varying stiffness
Jason Zarate, Sachem High School East, Farmingville, NY
Ruch Kopyto, Stella K. Abraham High School for Girls, Hewlett, NY

The Effect of Titanium Dioxide Nanoparticle Exposure on Cellular Migration, Proliferation, Morphology, and Collagen Contraction in Adipose-Derived Stem Cells
Nicolette Almer, Plainview-Old Bethpage John F. Kennedy HS, Plainview, NY
Kimia Ziadkhanpour, Plainview-Old Bethpage John F. Kennedy High School, Plainview, NY

Controlling Anti-Thrombogenic Properties of Polymer Surfaces Through Sterilization Techniques for the Development of Safer Medical Device Implantation
Paige Botie, Half Hollow Hills High School West, Dix Hills, NY
Yaakov Eiferman, Rambam Mesivta High School, Lawrence, NY

The Adverse Effects of Titanium Dioxide and Zinc Oxide Nanoparticle on Human Cervical Adenocarcinoma (HeLa) Cell Membranes and Ion Current Flow
Shoshana Guterman, Yeshiva University High School for Girls, Hollis, NY
Emma Zawacki, Smithtown High School East, St. James, NY

The Proliferation and Differentiation of Dental Pulp Stem Cells on Graphene/P4VP Composite Substrates
Aaron Argyres, Clayton High School, St. Louis, MO
Mingu Kim, Hickman High School, Columbia, MO

11:40 – 11:55 **Drug Delivery and Disease Detection**

Chairs: Jacob Wax, University of Pennsylvania; Tom Van Bell, The Wheatley School; Vianney Delplace, Institut Galien University of Paris

Functionalization of Gold Nanoparticles as Drug Delivery Agents for Treatment of Cryptococcosis
Allison Chowdhury, The Wheatley School, NY
Greta Huang, Commack High School, Commack, NY

The Effects of PLGA Nanoparticles and Surfactant on Endothelial Cell Cytotoxicity and Angiogenesis
Daphne Chen, Palm Harbor University High School, Palm Harbor, FL
Leandra Meraglia-Garcia, St. Anthony's High School, South Huntington, NY

Treating Cryptococcus Infections by Use of PLGA Nanoparticles Loaded with Novel Antifungal Drug BIBM
Luke Chen, Blue Valley High School, Stilwell, KS
Siavash Parkhideh, Ward Melville High School, East Setauket, NY
Vivek Subramaniam, Westborough High School, Westborough, MA

The Effects of Ultraviolet-B Exposure and Rutile Titanium Dioxide Nanoparticles on Cryptococcus-infected Macrophage Cells
Matthew Kempster, Mira Loma High School, Sacramento, CA

Creation and Optimization of a Potentiometric Biosensor for the Detection of Damaged Fibrinogen Molecules
Benjamin Khakshoor, North Shore Hebrew Academy High School, Great Neck, NY

11:55 – 12:00 **Virus/Bacteria Infection and Prevention**

Chairs: Alex Lee, Purdue University; Sooditi Sood, New York University; John Jerome, Suffolk County Community College

Titanium Dioxide Nanoparticles: An Effortless Path for Staphylococcus aureus to Infect Cells

Aaron Gochman, Sanford H. Calhoun High School, Merrick, NY

Antibacterial Properties of Phase Separated Polymer Blends and Graphene/Graphene Oxide

Allison Lee, Hauppauge High School, Hauppauge, NY

Jing Xian Wang, Centennial High School, Ellicott City, MD

Yongyi Zhao, Newton North High School, Newton, MA

12:00 – 12:10 **Dental Pulp Stem Cells**

Chairs: Yingjie Yu, Stony Brook University; Luidi Zhang, Stony Brook University

The Effects of Electrically Conductive Surfaces, Such as Poly(3-hexylthiophene), on Dental Pulp Stem Cell Differentiation

Evelyn Kandov, Yeshiva University High School for Girls, Holliswood, NY

Abraham Gross, Rambam Mesivta Highschool, Lawrence, NY

The effect of TiO₂ concentration on dental pulp stem cells using SPS and PB substrates

Min Seong Kim, Jericho High School, NY

Alec Silverstein, Biotechnology High School, NJ

Developing an Alternative Root Canal Filler to Stimulate Dental Pulp Stem Cell Proliferation and Differentiation

Ruiyi Gao, Lincoln Sudbury Regional High School, Sudbury, MA

Amanda Shi, Westlake High School, Westlake Village, CA

Gala Buffet Luncheon: WingWan of West Hempstead





The Garcia Center

Invites you to attend the

Annual Summer Symposium

of the

Research Scholars Program

on

Friday, August 9, 2013

10:00 am - 2:00 pm

in the

Student Activities Center, Ballroom A

Stony Brook University

10:00 am Coffee, Welcome, Student Musical Arrangments

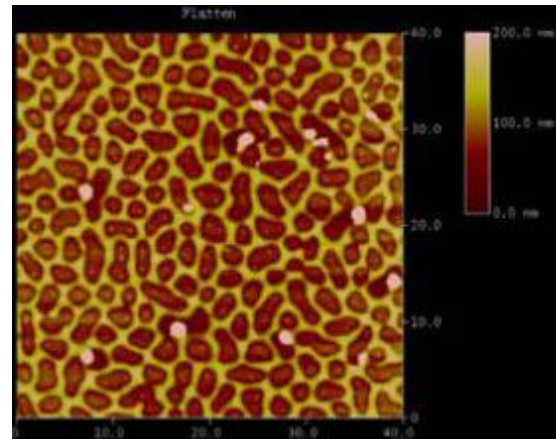
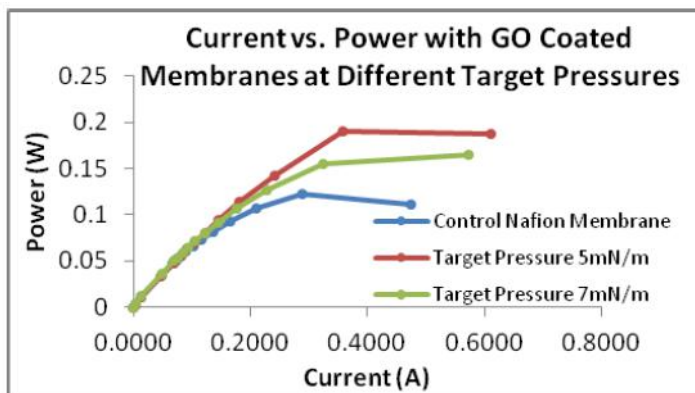
10:15 am - 12:15 pm Student Presentations

12:15 pm - 2:00 Formal Luncheon arranged by Wing Wan of West Hempstead, NY

Materials for Energy Generation

Chairs: Andrew Chen, Rice University; Weida Zhang, Stony Brook University; Benjamin Goldman, Queens College

Graduate Mentors: Zhenhua Yang, Hongfei Li, Cheng Pan



Investigating the ability of a photovoltaic system with battery backup to power life support in case of emergency

Alex Tang, Interlake High School, Bellevue, WA

Weida Zhang, Stony Brook University, Stony Brook, NY

Dr. Miriam Rafailovich, Dept. of Materials Science and Engineering, Stony Brook University

In recent times, powerful storms have knocked out power supply to many citizens, some of which rely on the essential electricity to power their life support units. While generators are available as backup power, they can run into problems and some are not designed to be run for 24 hours for two weeks, such as that of Gatlan Graham's during Hurricane Ike.¹ More recently, Brooke Ellison's generator ran hot for the two weeks when she was without power during Hurricane Sandy (E. Ellison, personal communication, July 18, 2013), a potential health hazard.

The goal of this investigation is to evaluate and apply a mobile solar STAR unit provided by Nextek, Inc. and Dynamic Supplier Alignment, Inc. towards powering critical loads of Brooke Ellison's house. The efficiency of the Bosch solar panels were tested through comparing the intensity of the photopic light coming from the Sun with the power output of the solar cells and the capabilities of the two types of batteries were analyzed for effectiveness through repeated cycling.

The STAR unit was provided and set up with the help of Nextek, Inc. and Dynamic Supplier Alignment, Inc. It consists of six solar panels, two sets of four AGM batteries from different companies, a wattmeter, a PureSine inverter, a solar charge controller, and a photometer. All of these elements were assembled into a mobile trailer unit with an external single phase 120V 30A outlet.

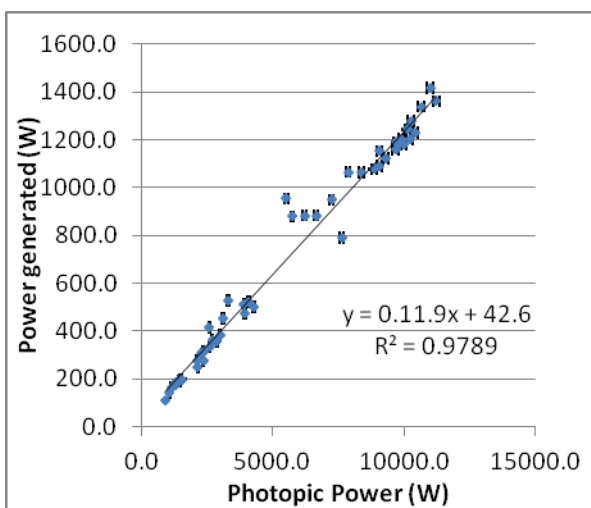


Figure 1. Power received from the Sun vs. Power generated by the solar panels.

Using the wattmeter, and later the Tristar interface, the investigation obtained several days worth of information spanning across sunny and cloudy days regarding the power output of the solar panels. For around 4 hours on sunny days, the power produced peaked 1,000W. The power produced on cloudy days depended on the amount of cloud cover. Data was also retrieved using the photometer at the same time as the wattmeter measurements to obtain photopic intensity readings. Calculating the efficiency between the energy from the sun and the energy produced yielded an efficiency of 11.9% efficiency as illustrated in Figure 1, contrasting with an expected efficiency of around 24% for monocrystalline silicon panels.²

The DEKA batteries were able to power the ventilator, fan, and space heater for around 10 hours. The Betta batteries were able to do so for over 10 hours. More testing is being carried out on the functionality of the batteries. Further testing of the batteries will be performed, especially to evaluate the damage done through the deep cycling of the batteries. Further research will be done to evaluate the properties of the provided batteries, and field tests will be conducted at Brooke Ellison's house, provided that the system will be able to interface with the power system of the house. Data will be gathered throughout the year to evaluate the feasibility of the system during all seasons and varying weather conditions.

¹ Associated Press. (2009, January 12). Keeping home life-support up during outages. *NBC News*.

² Zhao, J., Wang, A., Green M. A., & Ferrazza, F. (1998). 19.8% efficient "honeycomb" textured multicrystalline and 24.4% monocrystalline silicon solar cells. *Applied Physics Letters*, 73.

Graphene oxide coated Nafion membrane for enhanced performance in polymer electrolyte membrane fuel cells

Cameron Akker, Redmond High School, Redmond, WA

Andrew Chen, Rice University, Houston, TX

Cheng Pan, Brook University, Stony Brook, NY

Hongfei Li, Stony Brook University, Stony Brook, NY

Dr. Miriam Rafailovich, Stony Brook University, Stony Brook, NY

In the field of materials science, graphene oxide is a quickly emerging substance valued for its incredible chemical properties including high tensile strength, electrical insulating ability, and high thermal insulation¹. In regards to clean energy, hydrogen fuel cells are an effective alternative to traditional fossil fuels because of their clean by-products and relative efficiency. Using a combination of platinum and other co-catalysts, the efficiency of these fuel cells can be greatly improved². As the mechanism for the reaction in a hydrogen fuel cell is not thoroughly understood, true catalytic enhancement and improvement of fuel cell performance by other chemical means cannot be distinguished. Most of the current known co-catalysts for hydrogen fuel cells are metal alloys. Unfortunately, these metals are often expensive and subject to wear after extended use. Alternative co-catalysts are currently being researched including graphene oxide.³

The purpose of this research project to explore the effects of a graphene oxide coated Nafion membrane on power output in hydrogen fuel cells. The graphene oxide was put into a solution and deposited on the Nafion membrane by use of a Langmuir-Blodgett trough. The Nafion membrane was then tested in a single stack fuel cell against a control membrane with a hydrogen gas flow rate of 40ccm.

Graphene oxide was synthesized by a modified Hummers method in which graphite powder was chemically separated and exposed to strong oxidizers forming a paste. The resulting graphene oxide paste was allowed to dry in a vacuum until solid graphene oxide sheets were obtained. Graphene oxide sheets were then dissolved in a solvent solution made up of ethanol and water in a 1:3 ratio. The concentration of graphene oxide in the solvent solution was approximately 1mg/mL. The graphene oxide solution was spread on a water subphase at a rate of 1mL every 4 minutes with an initial concentration of 1mL for a total time of 36 minutes and final added volume of 10mL.

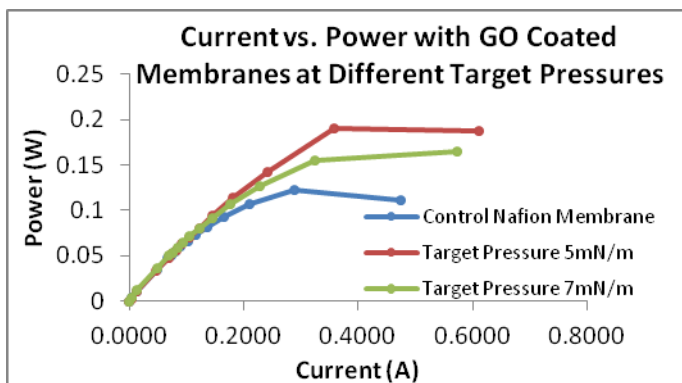


Figure 1: Current vs. Power graph for graphene oxide coated membranes with hydrogen gas flow rate of 40ccm

Two membranes were coated at a compression speed of 5mm/min and dip speed of 3mm/min using this process and target pressures of 5mN/m and 7mN/m. The two membranes along with a control, uncoated Nafion membrane were tested in a single stack hydrogen fuel cell for voltage and current at different levels of resistance, as indicated in figure 1. It was determined that the membranes coated in graphene oxide improved the power output in comparison to the control Nafion membrane.

Further research will be done to determine which specific target pressure produces the most effective layer of graphene oxide to enhance performance of the cell. Additionally, membranes coated in reduced graphene oxide will be made and tested in PEM fuel cells to determine what effect they have. TEM will be performed as well to examine the chemical structure of graphene oxide used in the coating.

¹Zhu, Y., Murali, S., Cai, W., Li, X., Suk, J.W., Potts, J. R., Ruoff, R. D. Graphene and Graphene Oxide: Synthesis, Properties, and Applications. *Advanced Materials* 2010; 22 (35): 3906-3924.

²Wang, L., Husar, A., Zhou, T., Liu, H. A parametric study of PEM fuel cell performances. *International Journal of Hydrogen Energy* 2003; 28: 1263-1272.

³Cote, L. J., Kim, F., Huang, J. Langmuir-Blodgett Assembly of Graphite Oxide Single Layers. *Journal of the American Chemist Society* 2009; 131(3): 1043-1049.

Improving Organic Polymer Solar Cell Efficiency via Active Layer Organization and the Incorporation of Graphene, Graphene Oxide, and Carbon Nanotubes

Kaveh Issapour¹, Krishana Raghubeer², Noah Davis³

Dr. Miriam Rafailovich⁴, Rebecca Isseroff², Cheng Pan⁴, Andrew Chen⁵

1) Syosset High School, Syosset, NY 11791 2) Lawrence High School, Cedarhurst, NY 11516 3) Earl L. Vandermeulen High School, Port Jefferson, NY 11777 4) Garcia MRSEC, SUNY Stony Brook, NY 11794 5) Rice University, Houston, TX 77251

Organic photovoltaics (OPV) offer a potentially more cost-effective alternative to their inorganic counterpart. However, the efficiency of OPVs are currently very low and must be increased in order for OPVs to become a viable source of alternative energy. The issues that are being addressed in this research are the unorganized active layer and the dissociation of excitons (electron-hole pairs).

Previous research has shown that the incorporation of a third polymer, such as polystyrene (PS), creates an ordered column structure, which creates a direct path through which the charges can flow¹. The P3HT arranges itself into a parallel alignment, while the PCBM shapes the structure into nano-columns, allowing more efficient exciton dissociation in conjunction with the improved charge transport. Incorporation of carbon allotropes, such as graphene and carbon nanotubes, has also shown an improvement in efficiency. The goal of this research is to combine both of these aspects, organizing the morphology while simultaneously synthesizing and incorporating various carbon allotropes.

Graphene oxide was synthesized using a modified Hummer's method, where 1.0 gram of high-purity powdered graphite was placed in a battery jar containing 23 mL of H₂SO₄(aq) in an ice bath. Then, while stirring, 0.5 grams of NaNO₃ and 3 grams of KMnO₄ were added. The GO paste was removed from the ice bath and stirred at approximately 35°C for an hour. 23 mL of DI H₂O was slowly added, raising the temperature to 95°C. The diluted suspension was maintained for 15 minutes above 60°C, and then diluted again with 35mL of warm water. The resulting suspension was treated with 2.5 mL 30% H₂O₂ and then washed with 10 ml 36% HCl. The filtrate was then washed six times with H₂O and dried in a vacuum oven.

Graphene was synthesized from graphene oxide (GO) through a simple, tabletop reduction. GO was

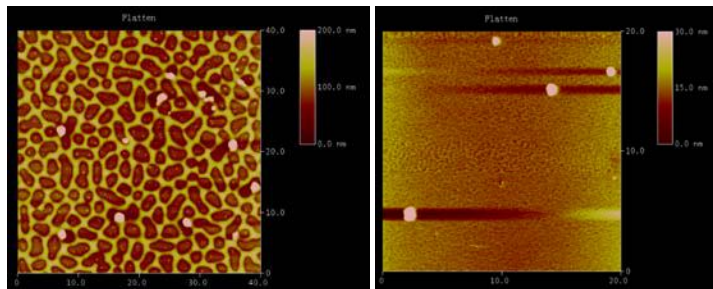


Figure 1: AFM scan of P3HT:PCBM shows a smooth, homogeneous film, whereas the image of P3HT:PCBM:PS shows on an ordered column structure.

suspended in a 25:75 ratio of ethanol and water and then sonicated for 30 minutes. The suspension was then centrifuged at 2500 rpm for 10 minutes. The supernatant was decanted and then the reducing agent NaBH₄ was added to the supernatant to a final concentration of 15 millimolar. The resulting solution was then allowed to stir overnight. This process was repeated with the presence of Potassium Chloroaurate (III) to create gold-functionalized graphene sheets.

Gold has been previously used to link organic molecules containing sulfur through a gold-thiolate bond². There are several future goals of this research. First is to incorporate our synthesized material, gold-functionalized graphene, into the active layer with the addition of sulfonated polystyrene, examining the morphology and the solar cell efficiency. Another option that will be examined is the incorporation of poly methyl methacrylate and carbon nanotubes, due to their affinity to each other. Finally, improving the hole transporting polymer is another path that will be investigated.

1 Segui J. et al. APS Bulletin. March 2008

2 Hannu Hakkinen. The gold-sulfur interface at the nanoscale. Nature Chemistry (2012) 4: 443–455

Effect of Nanoparticle Monolayer Coating of Nafion[®] Membrane on PEMFC Performance and Tolerance to Fuel Impurities

Rose Bender and Joshua Wende, Half Hollow Hills High School West, Dix Hills, NY
Hongfei Li, Cheng Pan, and Miriam Rafailovich, Dept. of Material Science and Engineering,
Stony Brook University, Stony Brook, NY

Hydrogen fuel cells are a very promising source of clean, renewable energy. Since water and heat are the only waste products of PEM fuel cells, they are being heavily researched as an alternative to fossil fuels. However, fuel cells are still far from ready for industrial application; their shortcomings include high costs, low efficiency, and a poor tolerance for fuel impurities.¹ The goal of this project is to investigate the effect of different nanoparticle monolayer coatings of the Nafion[®] membrane on the power output and efficiency of the fuel cell, using both pure hydrogen fuel and impure, mixed gas fuel.

The nanoparticles used were Au/Pt and Au/Pd alloys. A 1 mg/mL solution of nanoparticles in toluene was prepared and used in the Langmuir-Blodgett trough to deposit the nanoparticle monolayer onto the Nafion[®] membrane. An uncoated control membrane and one coated membrane for each nanoparticle were assembled into an H-tec fuel cell kit. Several variables were manipulated, including the flow rate of pure hydrogen fuel, the addition of varied rates of nitrogen at the anode, and the addition of carbon dioxide at both the anode and the cathode. For each test, voltage and current were measured at a range of different resistances, and power was calculated and analyzed in relation to current.

Preliminary tests of the flow rates of pure hydrogen revealed that 40ccm was the optimal rate for both coated and uncoated membranes; therefore, all further mixed gas tests were run at this flow rate. These pure fuel tests also revealed an increase in power for the coated membranes: 42% for Au/Pt, and 19% for Au/Pd. Tests of carbon dioxide at the anode revealed that increasing the flow rates of carbon dioxide decreases the power of the fuel cell, likely due to the conversion of carbon dioxide to the catalyst-poisoning carbon monoxide.² This poisoning effect, however, was diminished in the fuel cells with coated membranes, especially with the Au/Pd, as shown in figure 1. Adding nitrogen also decreased the power of the fuel cell, but the nanoparticles had little/no effect on the efficiency in this case.

Analysis of carbon dioxide and oxygen addition at the cathode is not statistically significant, due to large error caused by rapid dehydration of the membrane.

These results show promise for the use of a nanoparticle monolayer coating on the Nafion[®] membrane in increasing fuel cell efficiency, especially when carbon dioxide mixed fuel is used. Future studies include the investigation of other nanoparticles, such as Cu/Pt, to compare its effects to those of the other nanoparticles and of the pure membrane. Once this test is performed, we will have a better understanding of how to best improve the efficiency and impurity tolerance of PEMFCs and bring them closer to practical industrial applications.

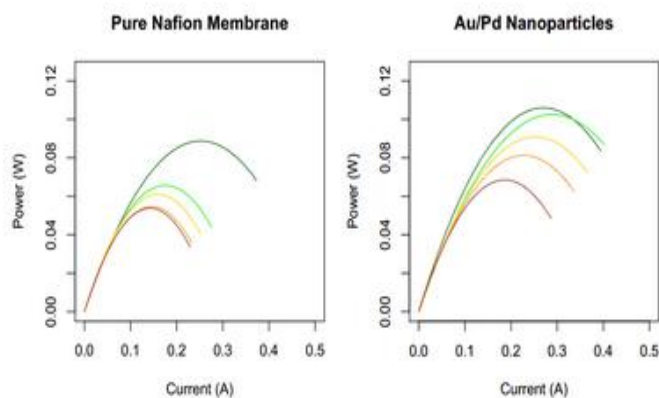


Figure 1: Power vs. Current curves for uncoated and Au/Pd coated membranes. Au/Pd greatly improved resistance to poisoning. Dark green = 0ccm CO₂; Light green = 10ccm CO₂; Yellow = 20ccm CO₂; Orange = 30ccm CO₂; Red = 40ccm CO₂

References:

- [1] U.S. Department of Energy. (2013, August 06). *Benefits and Challenges*. Retrieved August 6th, 2013
- [2] Nachiappan, N., Paruthimal Kalaignan, G., & Sasikumar, G. (2013). Effect of nitrogen and carbon dioxide as fuel impurities on PEM fuel cell performances. *Ionics*, 19. (351-354). doi:10.1007/s11581-012-0730-z

Optimization of Bulk Heterojunction Solar Cells via Phase-Separated Polymer Blends

Sharon Shu, Campbell High School, Smyrna, Georgia

Brian Zhong, Dougherty Valley High School, San Ramon, California

Zhenhua Yang, Dept. of Materials Science and Engineering, Stony Brook University

Cheng Pan, Dept. of Materials Science and Engineering, Stony Brook University

Dr. Miriam Rafailovich, Dept. of Materials Science and Engineering, Stony Brook University

Organic solar cells (OSC) are composed of photoactive polymer thin films as opposed to the metals of conventional solar cells. Much research has been done with regard to improving the active polymer layer of OSCs because of the lightweight, flexible nature of polymers and their relatively inexpensive cost. Bulk heterojunction (BHJ) solar cells contain multiple interfaces between the electron acceptor PCBM and the electron-donating, photoactive polymers P3HT and MEH-PPV. At these boundaries, charges separate and travel through self-assembled polymer columns¹ to the electrodes of the solar device, generating a current. The purpose of this project is to utilize various polymer blends in the active layer to produce greater morphology, voltage, and efficiency through phase-separation.

The polymer blends listed in **Table 1** were prepared by dissolving corresponding weights of each polymer in 1 mL of 1,2-dichlorobenzene. Glass slides coated with indium tin oxide (ITO) were first spin-coated with PEDOT:PSS in air, and then with a thicker layer of polymer blend. Aluminum electrodes were deposited onto the active layer using physical vapor deposition (PVD), and the devices were annealed in a vacuum oven. The photovoltaic performance of these devices was tested using a solar simulator with an AM1.5G filter under light with an intensity of 100 mW/cm². The morphology of the films were analyzed using atomic force microscopy (AFM) and transmission electron microscopy (TEM).

In terms of morphology and open-current voltage (V_{oc}), the devices yielded successful results. While the morphology of unblended P3HT film is generally flat and shows no column structures, the AFM images in **Figure 1** show that the addition of MEH-PPV enhanced the film's ability to phase-separate, with columnar structures up to 40 nm in height observed in **1b**. The blends of P3HT and MEH-PPV consistently resulted in higher V_{oc} of ~0.7 V compared to the 0.5 V to 0.6 V of the blends without MEH-PPV, which can

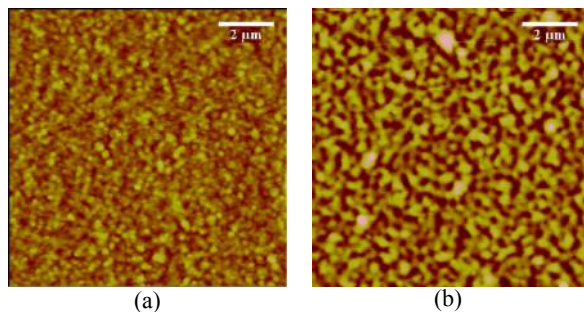


Figure 1: AFM Images of Polymer Blends

The domains of the PPV:P3HT:PCBM blends (b) show greater height difference indicated by the color contrast when compared to the P3HT:PCBM control (a).

be attributed to the greater phase-separation. Despite being lower in efficiency than pure P3HT devices, MEH-PPV holds great potential as a photoactive polymer due to its high voltage production and use as a catalyst for phase-separation. We plan to capitalize upon these qualities of MEH-PPV in the future while further raising the efficiency of our devices by focusing upon improving the current density and fill factor of the devices using means such as a lithium fluoride layer for greater electron transport

Blend	Ratio (mg/mL)	Efficiency (%)	J_{sc} (mA/cm ²)	V_{oc} (V)	FF (%)
PPV:P3HT:PS:PCBM	4:4:8:16	0.303	1.35	0.735	30.5
PPV:P3HT:PS:PCBM	4:4:16:16	0.194	0.84	0.765	28.6
PPV:P3HT:PCBM	4:4:8	0.329	1.92	0.735	23.3
PPV:P3HT:PCBM	3:6:9	0.258	2.10	0.595	20.6
P3HT:PS:PCBM	8:8:16	0.467	2.11	0.555	40.0
P3HT:PCBM	8:8	0.908	3.94	0.535	43.1

Table 1: Device Performance of Various Polymer Blends

The data obtained from the experiment reveals that polymer blends including MEH-PPV yield higher open current voltage, but lower current density (J_{sc}), fill factor (FF), and overall efficiency.

¹ Pan, C.; Li, H.; Akgun, B.; Satijia, S. K.; Zhu, Y.; Xu, D.; Ortiz, J.; Gersappe, D.; Rafailovich, M. H. *Macromolecules* **2013**, *46*, 1812-1819.

Gold platinum and copper platinum nanoparticles-coated Nafion membrane for enhanced performance in polymer electrolyte membrane fuel cells

Tuan Anh (“Thomas”) Lam, Loomis Chaffee School, Windsor, CT
Cheng Pan, Hongfei Li, Dr. Miriam Rafailovich, Dept. of Materials Science and Engineering,
Stony Brook University, Stony Brook, NY

Although a promising solution to our current energy crisis, hydrogen fuel cells currently have limited commercial use. One of the challenges faced in developing this technology is increasing the power output while keeping production costs at an acceptable level. Many past researches suggest that in addition to the much necessary but expensive platinum catalyst other highly catalytic and commercial viable materials can be installed into the cell to greatly increase the energy conversion rate to offset its commercial costs. The goal of this project is to maximally increase the energy output efficiency of hydrogen fuel cells using two nano-sized materials deposited on Nafion® membrane and determine whether one material is better and what the optimal coating for each material is.

Particularly, in this research project, two alloy nanoparticles, gold platinum and copper platinum, are synthesized using the two-phased Brust method¹ and then coated on the Nafion® membrane in layers with three different thicknesses based on data from their isothermal curves obtained using the Langmuir-Blodgett (LB) trough. Then these nanoparticles-coated membranes are in turn put into a stack of hydrogen fuel cell, which is tested for output current and voltage based on varying resistances. Tests are also performed on fuel cells with input oxygen gas at the cathode side. Control fuel cell tests are performed on those cells with pure non-coated Nafion® membranes. A comparison between experimental data and control data gives us both the exact output efficiency change caused by the nanoparticles and the optimal coating needed for each type of nanoparticle.

Data obtained so far suggests that for gold platinum nanoparticles, monolayer of the nanoparticles deposited on the Nafion® membrane obtained with the target pressure of 4 mN/m produces the maximum power output compared with control data and other experimental data with different target pressures. The highest power output of 4 mN/m gold platinum-coated membrane is .125 W, a visible 79% increase compared with maximum power output of .07 W produced by pure non-coated membrane, and 14% and 30% increase compared with maximum power output of 2 mN/m and 6 mN/m gold platinum-coated Nafion® membrane respectively.

TEM images have been performed on the two synthesized nanoparticles to determine average diameters of these nanoparticles, as seen in *Figure 1*. Data on copper platinum nanoparticles is still being obtained using the same procedure for gold platinum nanoparticles. Cyclic voltammetry tests will also be performed on these nanoparticles to determine their electrochemical and catalytic properties.

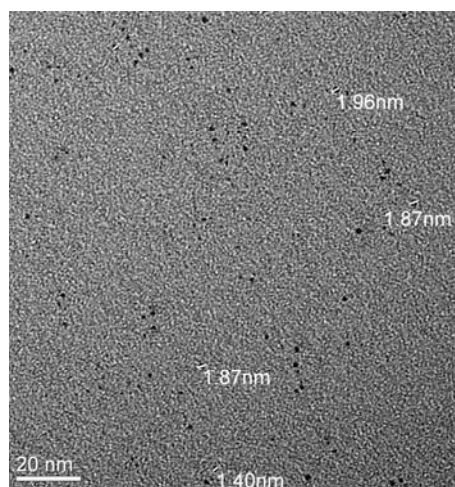


Figure 1: TEM image of copper platinum nanoparticles

¹ Brust, M., Walker, M., Bethell, D., Schiffrin, D. J., & Whyman, R. (1994). Synthesis of Thiol-derivatised Gold Nanoparticles in a Two-phase Liquid-Liquid. *J. Chem. Soc.*, 801-802.

Au/Pt nanoparticles for increasing CO₂ tolerance in PEMFCs

Tyler Dougan, The Blake School, Minneapolis, MN

Hongfei Li, Dept. of Materials Science, Stony Brook University, Stony Brook, NY

Cheng Pan, Dept. of Materials Science, Stony Brook University, Stony Brook, NY

Dr. Miriam Rafailovich, Dept. of Materials Science, Stony Brook University, Stony Brook, NY

Proton exchange membrane fuel cells (henceforth PEMFCs) are among the most viable technologies for energy storage, touted for their wide range of applications and “clean” operation. However, when the requisite hydrogen fuel is produced, it is often difficult to refine out other significant impurities, especially carbon dioxide.¹ The purpose of our research is to determine whether metal alloy nanoparticles could improve carbon dioxide tolerance by allowing for a side reaction that reduces the partial pressure of carbon dioxide, thereby purifying the fuel flow.

To investigate this, we coat a Nafion membrane with a monolayer of Au/Pt nanoparticles using a Langmuir-Blodgett trough. We then run a PEMFC fed with 40 cm³ min⁻¹ pure hydrogen, having determined that this flow rate produces the best performance. We add carbon dioxide to the hydrogen flow at the anode at flow rates of 10, 20, 30 and 40 cm³ min⁻¹, testing the nanoparticle-coated Nafion membrane as well as an uncoated membrane for control. We measure the composition of the output gas from the anode using gas chromatography.

The gas chromatograph used was not sensitive enough to measure the minute partial pressures of carbon monoxide (most likely less than 50 ppm²), which is acutely poisonous to the platinum catalyst, even in low concentrations. In Figure 1, we find that the nanoparticles do reduce the mole fraction of carbon dioxide in the anode output gas.

Because these nanoparticles were also found to improve cell performance, especially when carbon dioxide is added to dirty the anode gas flow, we contend that these nanoparticles act as sites for the carbon dioxide molecules to bind with, thereby decreasing the pressure of carbon dioxide within the cell. Because these nanoparticles will likely be less costly than removing carbon dioxide from an industrially-produced hydrogen supply, they could be incorporated into commercial PEMFCs to use impure hydrogen with little loss in performance. This research also opens avenues for investigation into the role of carbon monoxide, which should be present in small amounts with carbon dioxide. Unlike carbon dioxide, carbon monoxide actively poisons the cell, and its effects may also be diminished by nanoparticles.

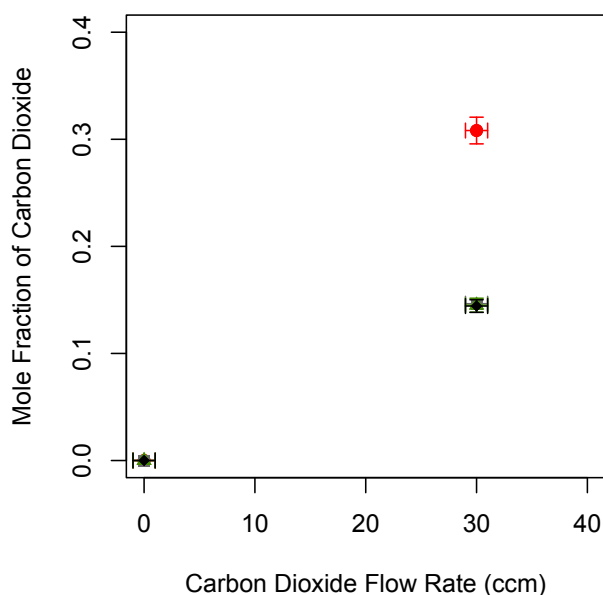


Figure 1: Plot of mole fraction of carbon dioxide in the anode output gas versus the carbon dioxide input flow rate in cm³ min⁻¹ (ccm). The Au/Pt nanoparticles (gray squares, which overlap with the black diamonds) clearly allow less carbon dioxide to escape into the output flow than does the pure Nafion membrane (red circles). The input flow composition is also plotted using black diamonds. Note that in some cases, the output concentration exceeds the input concentration of carbon dioxide because hydrogen was reacted within the cell.

¹Vijayaraghavan, K. & Soom, M. A. M. (2006). Trends in bio-hydrogen generation – A review. *Environmental Sciences*, 3(4), 255-271.

²Minutillo, M. & Perna, A. (2008). Behaviour modelling of a PEMFC operating on diluted hydrogen feed. *International Journal of Energy Research*, 32, 1297-1308.

Nanocomposites and Alloys

Chairs: Steven Krim, Stony Brook University; Julia Landsberg, Queens College; Julia Budassi, Stony Brook University

Graduate Mentors: Kai Yang, Yichen Guo, Zhihao Chen

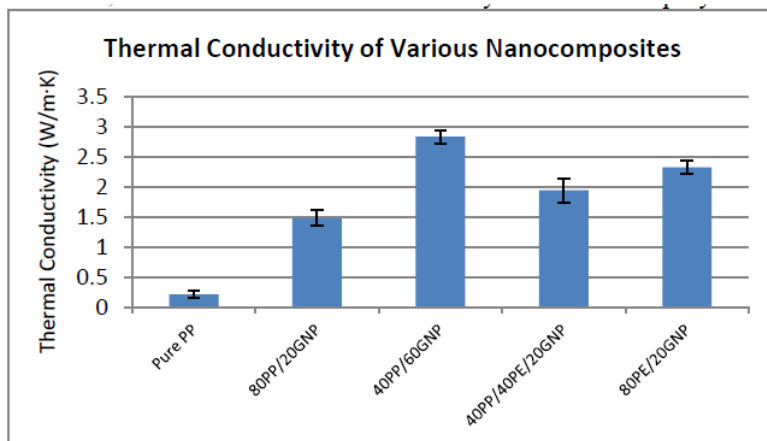
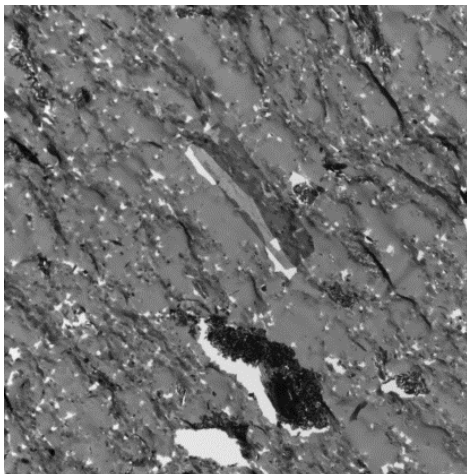


Figure 1 – Comparison of thermal conductivities.

Mechanical and Flame Retardant Properties of Styrene Copolymer Nanocomposites Using Different Clays

Brandon Prashad, Justin Silverman, South Side High School, Rockville Centre, NY
Yichen Guo, Stony Brook University, NY

Dr. Miriam Rafailovich, Department of Materials Science and Engineering, Stony Brook University, NY

Materials that are high impact and flame retardant are in high demand for both commercial and industrial use.¹ Some materials that provide these durable characteristics are metals that tend to be expensive, heavy and toxic with the addition of flame retardant chemicals. The goal of this project is to create copolymer blends that have high mechanical strength and flame retardant properties while still having the capacity to be non-toxic, cheap and light weight.²

In this study, a Brabender was used to mix the following polymers: High Impact Polystyrene (HIPS) and Acrylonitrile Butadiene Styrene (ABS) with the additives Halloysite, Cloisite 20A, and RDP Clay. Molds of each polymer blend were prepared for specific mechanical and flame retardant tests. The mechanical capabilities of the polymer blends were tested using the tensile test and Izod impact test. In order to study the polymer properties of the blends, the DSC and FTIR were used. The UL-94 flame test and cone calorimetry were used for studying the flame retardancy of our polymer blends.

It is evident that the pure samples of HIPS and ABS and the 90% HIPS/ABS 10% Halloysite had the highest results for both the Tensile and Impact Test. The DSC showed that as ABS nears its glass transition temperature it turns from rubber to rigid while HIPS turns from rigid to rubber. The FTIR provided data on the chemical composition of the ABS and HIPS polymers. The ABS and HIPS polymers were identical except that the ABS polymer contained an Acrylonitrile group: a polar hydroxide group. The TEM was used to examine the structure of the polymers. (Figure 1, 2). The flame test was successful after adding MgOH and ATH flame retardant agents which release water to cool down the system.

In conclusion, the tubular structure of the halloysite clay increased the tensile strength and the modulus of the polymer blends. The flame retardant agents MgOH and AlO₃ worked synergistically to make the polymers flame retardant. For future work, different concentrations of polymers and flame retardant agents will be blended to allow for flame retardant capabilities while maintaining mechanical strength.

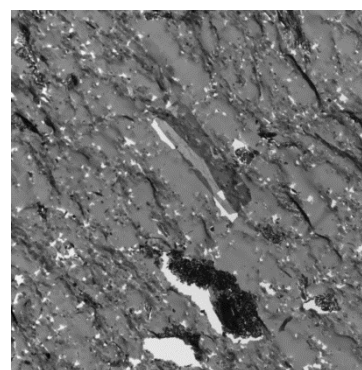


Figure 1- This is an image of the ABS polymer under the TEM.

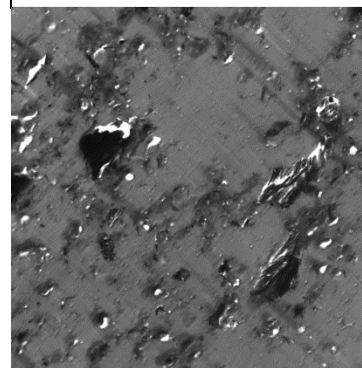


Figure 2- This is an image of the HIPS polymer under the TEM.

(1.) Rafailovich, M. H., Dr. (2010). Role of Surface Interactions in the Synergizing Polymer/Clay Flame. *Macromolecules Article*.

(2) Du, M. (2010). Newly emerging applications of halloysite. *Wiley Interscience*.

Erosion Testing of Plasma Sprayed Yttria-Stabilized Zirconia Coated Aluminum Substrates

Forrest Butensky, South Side High School, Rockville Centre, NY

Dr. Miriam Rafalovich, Dept. of Material Science and Engineering, Stony Brook University

Dr. Jason Trelewicz, Dept. of Material Science and Engineering, Stony Brook University

Gopal Dwidevi, Dept. of Material Science and Engineering, Stony Brook University

Mike Flynn, Stony Brook University

We live in an age where our technology is vital to our everyday lives. Some of this technology includes airplanes. Airplanes have revolutionized the way we travel. But our aerospace applications are vulnerable, and require many hours of maintenance. The parts of these applications that I am stressing are the turbine blades. They must be heat and erosion resistant and must protect against the elements. One revolutionary way to protect turbine blades is to coat them with a ceramic by using a process known as thermal spraying. Ceramics are very hard materials that are great at resisting heat and can protect against small debris. One ceramic in particular is known as yttria-stabilized zirconia (YSZ).^[1]

We performed a type of thermal spraying known as plasma spraying. This thermal spraying process consists of heating up a gas or mixture of gases to a very high temperature. This heating process turns the gases into a plasma state and is shot out of a jet torch. As this plasma jet is shooting out of the torch, the powder solution is inserted into the flame, which melts, and the melted deposits are shot onto a metal substrate, which in our case was aluminum (Figure 1). When producing these ceramic-coated substrates, conditions were changed in the production process to see how the microstructure and properties of the samples differentiated. The varying conditions included the amounts of hydrogen and argon used to produce the plasma, along with the current used to produce the plasma. Also, the rate at which the YSZ was fed into the plasma flume and the speed of the plasma jet moving left and right were other factors that were looked at while producing these samples.^[1]

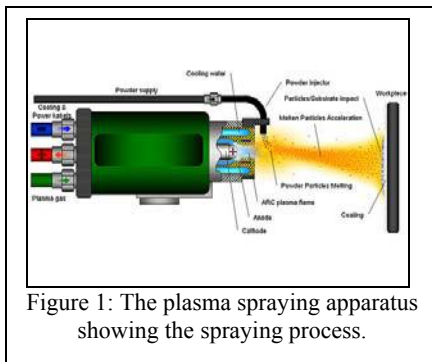


Figure 1: The plasma spraying apparatus showing the spraying process.

Once the samples were sprayed, they were tested to see how well they resisted erosion. They were blasted with alumina, which was released from a feeder. The samples were first weighed on a scale to obtain their initial masses. The samples were then blasted with the alumina for 2 minutes at a flow rate of 2 grams per minute and weighed again. This process took place two more times until their final masses were obtained. Once the mass differences were found we were able to find the erosion rate. It was found that the erosion rate for the samples was between .108 milligrams and .317 milligrams per gram of alumina shot at the samples.

Although my results didn't show a clear correlation for the erosion testing, a more thorough investigation is being taken place. It is possible to conduct many more tests in this field of engineering in the future. Erosion testing can be done on other samples. Another ideal test that can be conducted on the YSZ samples is the thermo-conductivity test. This test would allow us to see how much heat goes through the sample. The goal for this test would be for little to no heat to pass through the samples.

Vaidya, A., Srinivasan, V., Friis, M., Chi, W., & Sampath, S. (2008). Process maps for plasma spraying of yttria-stabilized zirconia: An integrated approach to design, optimization, and reliability. *Materials Science and Engineering*, 239-253.^[1]

Synergistic Effects of Graphene, Carbon Nanotube, and Copper Additives on the Thermal, Mechanical, and Flame Retardant Properties of Polypropylene

Joseph Cappadona, Lynbrook Senior High School, Lynbrook, New York

Ivy Ren, Thomas Jefferson High School for Science and Technology, Alexandria, Virginia

Kai Yang, Department of Materials Science and Engineering, Stony Brook University

Zhihao Chen, Department of Materials Science and Engineering, Stony Brook University

Dr. Miriam Rafailovich, Department of Materials Science and Engineering, Stony Brook University

In recent years, condensing boilers have become more popular due to their high efficiency ratings and ease of installation.¹ Heat exchangers in condensing boilers typically use aluminum alloys and stainless steel with thermal conductivities to transfer heat; thus, they need to be not only thermally conductive, but also flame retardant. However, due to their corrosivity, high cost, and maintenance requirements, metals are not optimal materials for use in heat exchangers. Due to their versatility, affordability, and processability, polymer composites have recently attracted attention as possible substitutes for heat exchangers. The goal of our research is to devise a polymer composite that conducts heat, withstands low pH environments, and prevents the spread of fire while remaining durable under stress.

Polypropylene (PP) has many attractive characteristics for use as a base polymer: tolerance to low pH environments, a relatively high melting temperature, and low cost. Similar to PP, polyethylene (PE) is inexpensive and resistant to corrosion.³ Although it has a slightly lower melting temperature, PE has stronger mechanical properties. Table 1 shows all of the blends that were tested.

As shown by Figure 1, the 40% PP and 60% graphene nanoplatelets (GNP) blend had the greatest thermal conductivity. It also showed an increase in thermal stability and achieved the highest possible rating of flame retardance (UL-94 Flame Test²), V-0, indicating that it will self-extinguish in less than 10 seconds without dripping when exposed to a 20mm flame. However, the addition of GNP dramatically decreased the polymer's tensile strength.

% by Weight			
PP	PE	GNP	CNT
—	100	—	—
—	80	20	—
100	—	—	—
80	—	20	—
60	—	35	5
60	—	40	—
40	—	60	—
40	40	20	—
% by Volume			
PP	Cu	GNP	
97	3	—	
90	10	—	
80	10	10	
80	20	—	

Table 1 – The various polymer blends tested in this study.

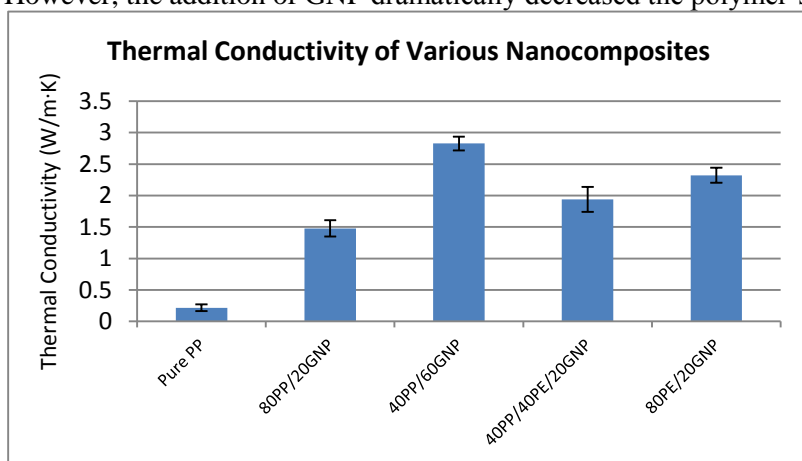


Figure 1 – Comparison of thermal conductivities.

More polymer blends will continue to be tested based on the literature. Copper has been shown to contribute greatly to thermal conductivity^{3,4} and will therefore be incorporated with graphene to try to enhance thermal conductivity without sacrificing mechanical properties. Carbon nanotubes will also be incorporated with graphene to improve mechanical properties while maintaining high thermal conductivity and flame retardance.

¹ Condensing boilers. (2012, September 25). Retrieved August 6, 2013, from The National Energy Foundation website: <http://www.nef.org.uk/energysaving/boilers.htm>

² UL 94, the standard for safety of flammability of plastic materials for parts in devices and appliances testing. (n.d.). Retrieved August 6, 2013, from Underwriter Laboratories website: <http://www.ul.com/global/eng/pages/offering/industries/chemicals/plastics/testing/flame/>

³ Boudenne A, Ibos L, Fois M, Majesté J, Géhin E. Electrical and thermal behavior of polypropylene filled with copper particles. *Composites Part A: Applied Science and Manufacturing*. 2005;36(11):1545-1554.

⁴ Molefi, J. A., Luyt, A. S., & Krupa, I. (2009, May 19). Comparison of the influence of Cu micro- and nano-particles on the thermal properties of polyethylene/Cu composites. *eXPRESS Polymer Letters*, 3(10), 639-649. doi:10.3144/expresspolymlett.2009.80

A multi-scale simulation: examining thermal conductivity of polymers enhanced by nanofillers of different geometries

Joseph Jacob¹, Dilip Gersappe², Miriam Rafailovich², Ning Sun³, Di Xu³, Kai Yang³

¹The Wheatley School, Old Westbury, NY

^{2,3}Department of Material Sciences and Engineering, Stony Brook University, Stony Brook, NY

In the recent decades, research has shown that nanofluids, fluids mixed with nanostructures, have thermal conductivities that are markedly higher than that of the fluid's original state^[1]. Past research has also shown that the most optimal types of nanostructures for this purpose are carbon-based, such as carbon nanotubes (CNT) and graphene^[2]. Since graphene is the more thermally conductive of the two, much research has been directed towards the effect of graphene on the thermal conductivity of certain polymers. This research on graphene has been conducted through both simulations and experiments, but there is difficulty with simulating graphene, especially in molecular dynamics. However, simulating the thermal conductivity of a nanocomposite, constructed from graphene and some other polymer, would offer the opportunity to calculate an accurate approximation of the nanocomposite's new thermal conductivity. Furthermore, the optimized geometry of the graphene is, i.e. as a sheet, tube, etc., has not been extensively researched because most research in the category has been conducted in a two-dimensional system.

This research will be split into two phases: molecular dynamics and the Lattice Boltzmann method (LBM). The molecular dynamics portion will be simulated in a program called LAMMPS (Large-scale Atomic/Molecular Massively Parallel Simulator) which will create an arbitrary polymer in the shape of a sphere and two different geometries of graphene (sheets and nanotubes) to ultimately find the nanocomposite's thermal conductivity and use the coordinates of the atoms in an equilibrium morphology, shown in Figure 1, for the LBM portion of the project, coded in a program called Palabos.

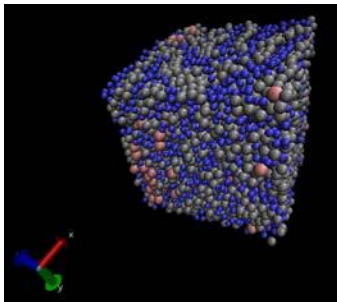


Figure 1: An example of a morphology typically derived from LAMMPS

LBM was originally conceived as a tool for computational fluid dynamics, but since then, its uses have been expanded to a variety of simulations, especially gas and heat diffusion. Every molecule in the system can be represented by a node on the lattice used by LBM, and once the system starts running, the collisions will be modeled by the Bhatnagar-Gross-Krook (BGK) collision model^[3]. The LBM portion of the research will also provide the system's thermal conductivity, but its true purpose is to provide the experiment at a much larger scale that LAMMPS cannot compute.

No results for the research have been collected yet; however, it is planned to have this research be conducted extensively in order to fully model the thermal conductivity in this nanocomposite and also find the optimal geometry for the nanofiller, graphene, associated with the nanocomposite. Research may also be taken into a more intensive state by examining the phonons of these solids and getting a more accurate view of why thermal conductivity increases in these nanocomposites.

[1] Jafarpur, K., & Javanmardi, M. (2013). A molecular dynamics simulation for thermal conductivity evaluation of carbon nanotube-water nanofluids. *Journal of Heat Transfer*, 135(4)

[2] Han, Z., & Fina, A. (2011). Thermal conductivity of carbon nanotubes and their polymer nanocomposites: A review. *Progress in Polymer Science*, 36(7), 914-944

[3] Wager, A. (2008) A practical introduction to the Lattice Boltzmann method. Unpublished manuscript, Physics, North Dakota State University

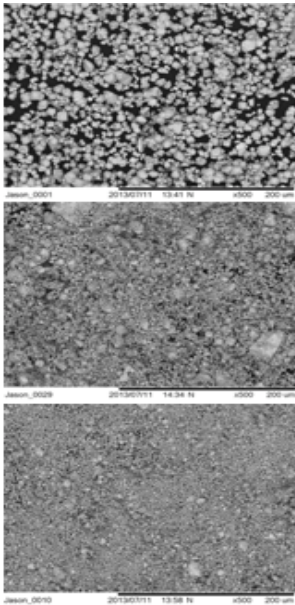
Nanocrystalline tungsten alloys for self-sharpening kinetic energy penetrators

Miriam Friedman¹, Brian Tackett², Olivia Donaldson³, Dr. Jason Trelewicz³
¹HAFTR High School, NY ²University of Pittsburgh, PA ³Stonybrook University, Department of Materials Science & Engineering, NY

Tungsten has long been sought as a potential penetrating material for the replacement of depleted uranium due to its high-density, corrosion resistance and low cost. The current materials used are far more expensive and are harmful to those producing them—since they are uranium based, and are thus toxic—and tungsten is believed to behave similarly without the extra monetary and health risks. Additionally, at high strain rates uranium fragments, promoting enhanced penetration efficacy; tungsten, on the other hand, deforms uniformly and does not have behave the same way. However, with a refined grain size (<100nm), tungsten begins to have a self-sharpening effect similar to that of uranium based materials.

Nanocrystalline metals are often unstable; their grains grow rapidly (even at low temperatures, making them unsuitable for usage), but alloying has been found to improve stability in certain systems¹. The Tungsten (W)-Titanium (Ti) system has demonstrated a substantial degree of stability, making it a promising candidate for a base alloy design for potential materials. W-Ti alloy would, however, be problematic due to its relatively low density of 16 g/cc (below 18 g/cc), making it unsuitable to be used as a

Fig 2: SEM: W with increasing milling time (0 → 12 hrs)



kinetic energy penetrator. Therefore, this design matrix begins with a base W-Ti composition and seeks to develop a two phase system utilizing other stable nanocrystalline alloys (based on the results of figure 1) in attempt to retain the properties of the alloyed elements while increasing density.

Statistical thermodynamic framework (figure 1) of the W-Ti system stands as the basis for design. Stage one of design models included binary systems of W-Ti, W-Nickel (Ni), W-Chromium (Cr), and W-Manganese (Mn) since these are believed to be stable in the nanocrystalline form at high temperatures. Stage two consisted of a ternary composition alloy in which W-Ti, again, stood as the base and compositions of Cr, Mn, and Ni were varied. Currently, a dual phase binary alloy seems ideal to the density and grains size requirements allotted for developing this kinetic energy penetrator.

With increased milling time on the planetary mill the powder begins to exhibit a high degree of fineness (figure 2) and its potential penetration ability enhances. Thus, the parameters were developed: 550 rpm, twelve- hour milling time, a five to one ball to powder mass ratio (using tungsten carbide balls with a 5mm diameter.) Analysis consisted largely of energy dispersive X-ray spectroscopy (EDS), scanning electron microscope (SEM) and X-ray diffraction (XRD) to determine grain size, plane orientation, and alloy composition based on spectra.

Enhanced tungsten alloys would have immediate implications for defense and energy markets where component functionality relies heavily on the performance of high-density materials.² In the defense arena in particular, munitions are needed that offer superior performance at a reduced cost and have minimal environmental impact. Possible applications include national defense as army piercing rounds, and shape charges in the oil and gas industries.

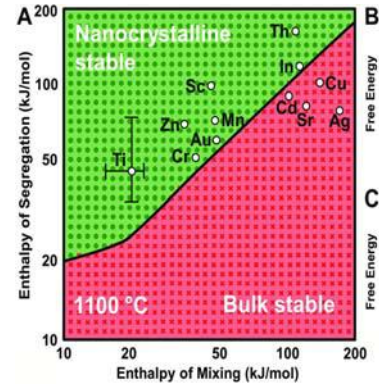


Fig. 1. The nanostructure stability map for Tungsten based alloys at 1100° C¹

¹ Tongjai Chookajorn, Heather A. Murdoch, & Christopher A. Schuh. "Design of stable nanocrystalline alloys" Department of Materials science and Engineering, *Science* VOL 337 (2012)

² Wei, Q.; Zhang, H.T.; Schuster, B.E.; Ramesh, K.T.; Valiev, R.Z.; Kecskes, L.J.; Dowding, R.J.; Magness, L.; Cho, K. *Acta Materialia* 2006, 54, 4079-4089

The Study of the Effects of Morphology and Porosity on Charge Capacity and Charge Rate of Graphite Anode Systems Using the Lattice Boltzmann Method

Varun Mohan¹, Ning Sun², Dilip Gersappe³, Miriam Rafailovich⁴

¹The Harker School, San Jose, CA

^{2,3,4}Department of Materials Science and Engineering, Stony Brook University, Stony Brook, NY

Lithium-ion batteries (LIB) have become crucial in commercial electronics for their capacity to efficiently charge and discharge devices. Although there are a variety of materials, namely metal oxides, used for the positive electrode, the cathode, ever since 1973¹, the predominant material for the negative electrode, the anode, is graphite. Moreover, graphite is an ideal anodic material due to its low cost as well as its interfacial and structural stability¹. However, one widely studied topic for LIB pertains to the suppression of dendrite formation, occurring on the anode material during the saturation of graphite, causing safety hazards and unstable charge/discharge cycles². Furthermore, the study of the morphology of the anode can reveal deep insight into how to maximize charge capacity and charge rate before the first saturation state of the graphite. The goal of this project is therefore to determine such an optimal structure for various graphitic systems, namely 2D models, 3D models, and core/shell models.

The approach taken to solve this complex problem employs a powerful tool, known as the Lattice Boltzmann Method (LBM) using the BGK collision operator. The method is a way to simulate fluid dynamics by placing a continuous fluid on a discrete lattice, storing the state of a fluid. However, over time, the capabilities of LBM have been adapted to other fields, including electromigration³.

In order to simulate the system, we also define the model as well as its environment. The system is first split into 3 components, namely the electrolyte, electrode, and the interface. Within the electrolyte, the processes of diffusion and electromigration affect the ion flow. In the electrode, the ions react with the graphite under the Butler-Volmer relation. Finally, the interface movement is governed by a first degree kinetics equation. The system was developed using C++, using the Palabos library, which specializes in LBM and facilitates the parallelization of the code. The total charge capacity was determined by summing up the current values at each time step until the first saturation point.

The results validate that LBM functions properly in simulating the system. We see this through the current vs. time graph for each system, which follows experimental trends. Moreover, initially, the current increased as a result of unreacted carbon, but over time started to decrease due to a diminished concentration gradient at the liquid-solid interface, leading finally to a steady state. For the simple 2D model, the capacity per node is an increasing function with respect to volume fraction. However, for the varying porosity model, there is a local maximum for capacity at a volume fraction at 70% as seen in Figure 1, due to the increased capacity at the surface and reduced pores within the structure. Finally, 3D results also resemble those of 2D.

The results have shown to our knowledge for the first time that LBM can model the charging process of a LIB. The result from Figure 1 indicates that for a controlled porous morphology, a high capacity can be achieved at high porosities. In the future, we shall study the effects of parallelization, interfacial area for 3D, and the composite model.

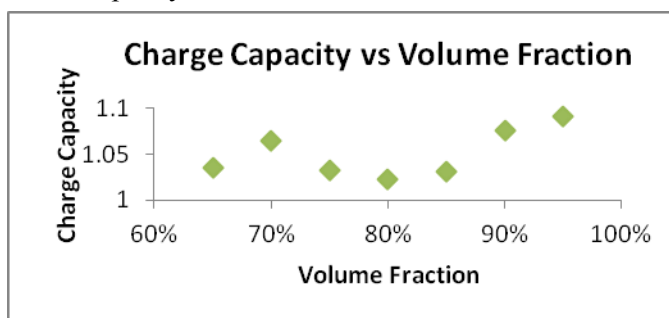


Figure 1: The Relationship between Charge Capacity and Volume Fraction for a Controlled Porous Structure.

¹ Kumar, Prem, Sri Devi Kumar, and Manuel Stephan. (2009). Carbonaceous anode materials for lithium-ion batteries - the road ahead. *Journal of Indian Institute of Science*, 89(4), 393-423.

² Bernard, Marc-Olivier, Mathis Plapp, and Jean-François Gouyet. (2003). Mean-field Kinetic Lattice Gas Model Of Electrochemical Cells. *Physical Review E* 68(1), 1-14

³ Chai, Zhenhua, Zhaoli Guo, and Baochang Shi. (2007). Study Of Electro-osmotic Flows In Microchannels Packed With Variable Porosity Media Via Lattice Boltzmann Method. *Journal of Applied Physics* 101(10), 104913.

Novel 2D and 3D Printing Technologies; Unusual Applications of Electrospun Fibers

Chairs: Monika Batra, Stony Brook University;
Rachel Yang, Cornell University; Aatman Makadia;
Timothy Hart, Stony Brook University

Graduate Mentors: Joe Miccio, Shan (Harry) He

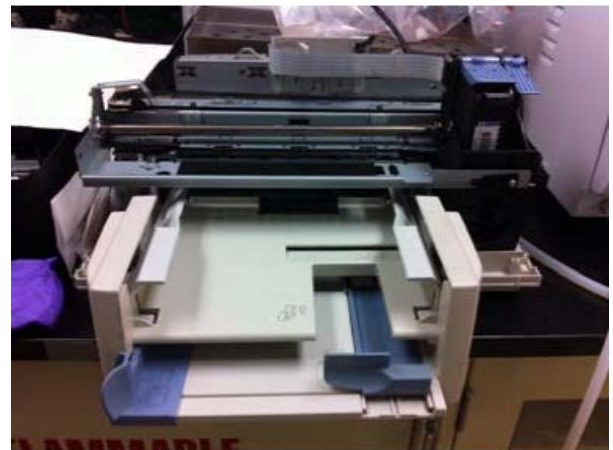
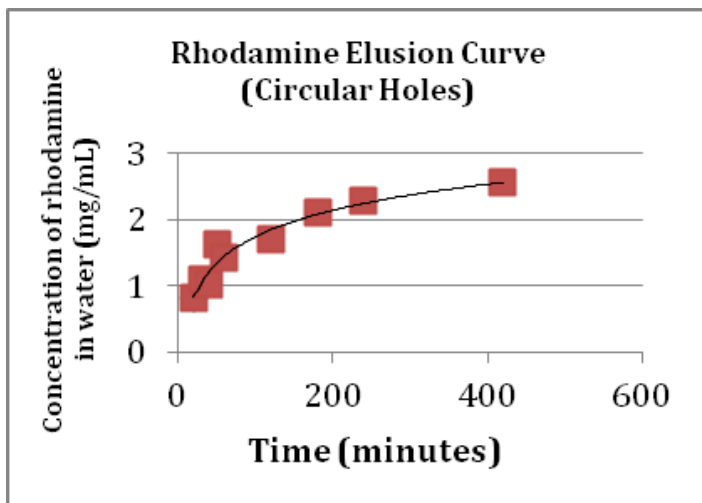


Figure 1: Modified HP Deskjet 890c printer that was utilized for cell printing

Using Three Dimensional Printing to create a Drug Eluting Scaffold

David Levi¹, Hillel Lerner¹, Fan Yang², Dr. Miriam Rafailovich², Dr. Michael Gouzman³

Rambam Mesivta High School¹, Stony Brook University, Department of Materials Science and Engineering², Stony Brook University, Department of Electrical and Computer Engineering³

In the past few years, Three Dimensional (3D) printing has risen in prevalence. One aspect of 3D printing on the rise is the design and printing of biocompatible scaffolds. Today, it appears advantageous to 3D print scaffolds as bone replacements, which may be able to solve targeted problems.¹ Moreover, certain biomaterials with specific components may be able to effect specific cell actions, such as chemotaxis, depending on their dosage and delivery system.² The goal of this project is to design and 3D print a prototype of a porous scaffold which contains a hydrogel which elutes the drug melatonin, used to help people who are suffering from bone loss.

We began experimentation with an UP! Plus 3D Printer©. We designed scaffolds using AutoCAD, 3D printed them and loaded them with a hydrogel that contained a mock drug, rhodamine. We measured how the rhodamine eluted from the hydrogel in the scaffold into DI water with the UV Visual Spectrophotometer. We created a rhodamine standard curve in order to extrapolate the concentration of rhodamine based on the measured absorbance of a sample. Using the Makerbot Replicator 2, which printed in PLA (poly lactic acid), we created our new scaffolds on AutoCAD. Our designs were boxes 1cm x 1cm x 3mm, with 25 circular holes pushed through the box, one with circles and one with squares. We figured out an optimal concentration of .16 mg rhoadamine/ mL hydrogel, with a 3:1 hydrogel: mTG ratio, which caused a high level of cross linkage. For our control we used a gel without a scaffold. We left the samples for 7 hours, and took regular measurements. For our design with circular holes, we got a curve of $y = 0.5705\ln(x) - 0.8866$, and $R^2 = 0.9498$, see figure 1.a. For our design with square holes, we got a curve of $y = 0.7047\ln(x) - 1.574$ and $R^2 = 0.9388$, see figure 1.b.

For future work, we must overcome one major problem. When an ABS scaffold is placed in an Autoclave for sterilization, it loses its structural stability. To fix this, we will try to create a nanocomposite of ABS and a mineral or polymer that has a glass transition temperature high enough to withstand the heat of the autoclave. Eventually we hope to create a working prototype of a 3D printed drug eluting scaffold.

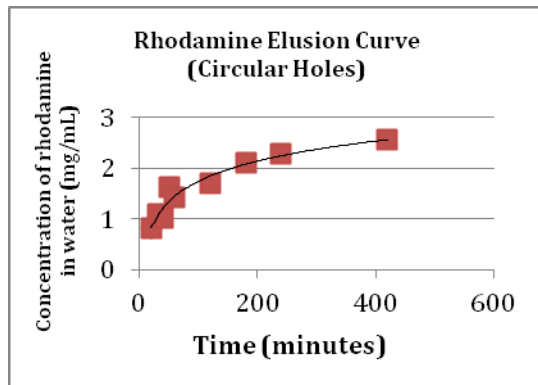


Figure 1.a. $y = 0.5705\ln(x) - 0.8866$, $R^2 = 0.9498$

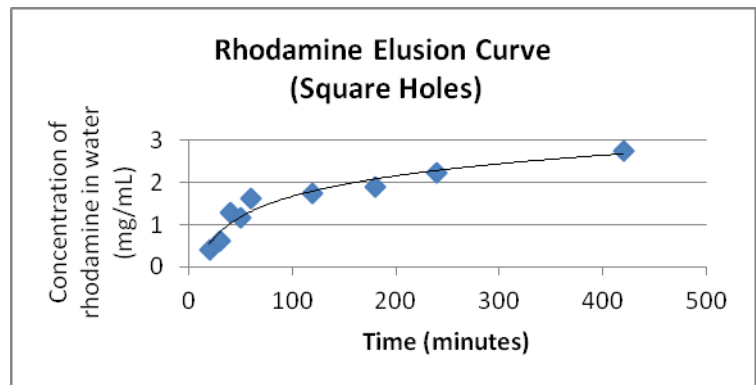


Figure 1.b. $y = 0.7047\ln(x) - 1.574$, $R^2 = 0.9388$

¹ Wang Bo, Ming et al. (2013), Study on Artificial Bone Scaffolds with Control Release of Drugs by Low-Temperature Rapid Prototyping Technology, *Advanced Materials Research*, 647, 269-277

² Vorndran, Elke et al. (2010), Simultaneous Immobilization of Bioactives During 3D Powder Printing of Bioceramic Drug-Release Matrices, *Advanced Functional Materials*, Volume 20, Issue 10, 1585-1591

Inkjet Printing of Human Dermal Fibroblasts and RK13 Cells for Applications in Tissue Engineering

Leeson Chen, Palm Harbor University High School, Palm Harbor, FL
Monika Batra, Fan Yang, Weida Zhang, Miriam Rafailovich, Department of Materials Science and Engineering, SUNY Stony Brook, Stony Brook, NY
Rachel Yang, Cornell University, Ithaca, NY

With modern medicine surging in demand and diversity, there is a mounting market for organ tissues created from stem cells. The most common method of growing these stem cell tissues is by seeding the cells manually; however this process can be challenging and tedious. An emerging and promising technology is the designing of specialized printers that are able to print cells in two-dimensional patterns, just as a normal desktop printer would print ink.¹ The goal of this project is to modify a conventional inkjet printer and cartridge so that it will print a variety of cells in programmed patterns onto Kapton film, and for the printed cells to survive in an incubator on the Kapton sheet. The printer modified was an archaic Hewlett Packard (HP) Deskjet 890c printer (Fig. 1), which used an HP 51645A ink cartridge. The cartridges were flushed out thoroughly with water, sonicated for at least three hours, rinsed periodically and then sterilized with 70% ethanol. For printing, a cartridge was loaded with no more than 10 ml of RK13 (rabbit kidney) cells or fibroblasts in the DMEM medium at a concentration of 1×10^5 cells/ml. Microsoft Word 2003 was used to create a square grid pattern, which was printed onto a piece of Kapton film attached to a sheet of standard 8.5 by 11 inch paper. The cells printed on Kapton

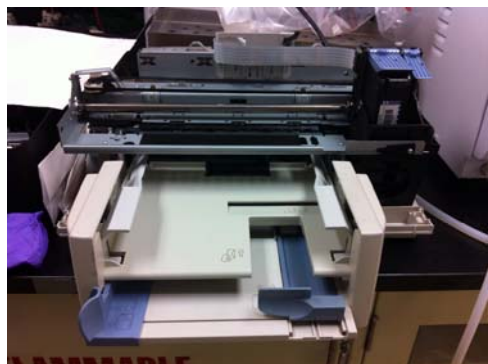


Figure 1: Modified HP Deskjet 890c printer that was utilized for cell printing

film were observed under an optical and fluorescent microscope using a live-dead stain, which determined cell viability after printing. The modified printer successfully printed RK13 cells and fibroblasts in 1×10^5 cells/ml concentrations separately onto Kapton, and the cells continued to survive under incubated conditions. However, the cells did not to adhere to the Kapton film when liquid medium was introduced. Two hydrogels of 5% and 7% concentration raised more difficulty in making the Kapton film adhesive, as the printer damaged the gel layer too severely to observe cells. However, the RK13 cells that were seeded onto the Kapton paper successfully adhered and survived, based on healthy cell morphology observed under the fluorescent microscope. Although definitive results were not yet achieved, the prospect of printing stem cells with an inexpensive modified printer would propel the stem cell tissue engineering field forwards by making stem cell tissues accessible and faster to create. The currently unresolved issues include printing on electrospun fibers, hydrogels, and glass slides by further modifying the printer's mechanics. Specialized software for designing patterns to print, as opposed to a word processor, would give more versatility to the structures. A functional printer that printed different designs could test whether stem cells grow better in certain arrangements. The transition of this technology to 3D printing could in time lead to printing entire organs from a machine.

¹ Xu, T., Jin, J., Gregory, C., Hickman, J. J., & Boland, T. (2005). Inkjet printing of viable mammalian cells. *Biomaterials*, 26, 93-99.

Novel Cimex Lectularius Trapping Mechanism Using Electrospinning Technology

Michal Leibowitz, Yeshiva University High School Girls, **Jacob Plaut**, Rambam Mesivta High School for Boys, **Daniel Rudin**, Half Hollow Hills High School West, **Timothy Hart**, Stony Brook University, **Shan He**, **Linxi Zhang**, **Miriam Rafailovich**, Stony Brook University Materials Science Department,

The Cimex lectularius is an insect commonly known as the bed bug. In recent years, there has been a resurgence of bed bug infestations in part due to their increased resistance to conventional insecticides.¹ This has led to a widespread demand for a cost-effective, efficient, and permanent solution. The purpose of this research project is to design and test a novel Cimex lectularius trapping mechanism using electrospinning technology. We hypothesized that when spun onto an appropriate substrate, the fine microfibers generated during electrospinning by the interactions of the electrical current with the polymer-based solution could create a web-like configuration ideal for mechanically trapping bed bugs. Various parameters influence the morphology and diameter of the electrospun fibers, including the concentration, surface tension, and viscoelasticity of the solution as well as the voltage, stock solution feed rate of the electrospinning apparatus.² We electrospun solutions of polystyrene (PS), polylactide (PLA), and polybutylene adipate-co-terephthalate (PBAT), onto standard printer paper as well as onto corrugated aluminum foil. Optical microscopy allowed us to analyze the diameter and configuration of the microfibers. Additionally we tested various trapping apparatus with bed bugs to observe their behavior and the relative effectiveness of each trap. In observing the behavior of the bed bugs, we found that bed bugs favor rough surfaces over smooth surfaces. The bed bugs use their antennae to test the substrate before stepping on it. When the substrate was aluminum, the bed bugs stayed on the paper stage away from the plastic box, but did not enter the trap itself. Bed bugs were more likely to enter the trap when the substrate was paper, presumably because they preferred the rough surface. In addition, the nocturnal bed bugs flocked to the dark crevices between the paper stage and the trap itself, also crawling under trap at some points.³ Noting this preference for darkness, we created a new trap using a corrugated substrate inserted between two flat pieces of paper. Compared to traps utilizing an open-faced structure which caught an average of 0.4 bed bugs over the course of five days of trials, the corrugated sandwich based trap caught an average of six. As is shown in the image above, we also found that when electrospun onto a corrugated aluminum substrate, polystyrene solutions of 12% concentration in 50 % tetrahydrofuran (THF) and 50 % dimethylformamide (DMF) form fibers most effective in immobilizing bed bugs by tangling the bed bug's six hooked legs, as is shown in Figure 1. These results present a commercially viable method for trapping bed bugs because of the effectiveness of the trap and relatively low cost of the materials. Our attempts to replicate the success of this solution using recycled polystyrene from packing peanuts shows promise. Additionally, we believe that in the future, a similar electrospun apparatus may be used to trap insects other than bed bugs.

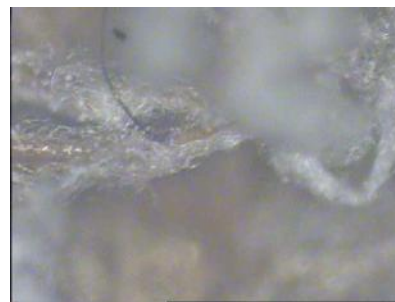


Figure 1: Optical microscope image of four bed bug legs tangled in electrospun fibers at 5x magnification

¹ Joint Statement on Bed Bug Control in the United States from the U.S. Centers for Disease Control and Prevention (CDC) and the U.S. Environmental Protection Agency (EPA), http://www.cdc.gov/nceh/ehs/Publications/Bed_Bugs_CDC-EPA_Statement.htm

² Ji, Yuan, Bingquan Li, Shouren Ge, Jonathan C. Sokolov, and Miriam H. Rafailovich. "Structure and Nanomechanical Characterization of Electrospun PS/Clay Nanocomposite Fibers." *Langmuir* 22 (2006): 1321-328. Web. 7 Aug. 2013.

³ Reis, Matthew Dougals. "An Evaluation of Bed Bug (*Cimex Lectularius* L.) Host Location and Aggregation Behavior." *Vt.edu*. N.p., 1 Oct. 2010. Web. http://scholar.lib.vt.edu/theses/available/etd-12102010-105743/unrestricted/Reis_MD_T_2010.pdf

Micro-Scale Engineering a Novel Tattoo Ink Removable by Ultrasound

Rohit Mehandru¹, Miriam Rafailovich², Jonathan Sokolov², Joseph Miccio^{3,5,8,9}, Xavier Marinaro⁴, Aatman Makadia⁵, Satya Makadia⁶, Suditi Sood⁷

¹Roslyn High School, ²Stony Brook University Dept. of Materials Science & Engineering, ³Stony Brook University School of Medicine, ⁴Cornell University, ⁵Stony Brook University Dept. of Bioengineering, ⁶Hofstra University, ⁷New York University, ⁸University of Pittsburgh, ⁹SonInk

According to the Harrison Poll in 2012, 21% of all adults living in the United States have at least one tattoo and 14% of these adults claim they regret getting said tattoos.¹ Current tattoo removal techniques mainly consist of Q-Switched lasers which utilize laser light energy to target specific chromophores leading to the generation of excess heat. This heat destroys the chromophores as well as surrounding fibroblasts in the dermis, resulting in significant unneeded tissue damage. This form of tattoo removal is also highly ineffective, only removing approximately 75% of most tattoos while costing thousands of dollars.² As a result, there is a growing need for precise and inexpensive tattoo removal methods that can target ink without dermal injury.

In order to achieve this we sought to engineer tattoo inks comprised of water soluble dye encapsulated in biostable polymeric microparticles as seen in Figure 1. First, dye molecules dissolved in a small amount of water are mixed with polymethyl methacrylate (PMMA). Second, sonication creates a primary emulsion of microdroplets of water containing ink within the bulk oil phase. Third, homogenization creates a double emulsion – droplets of organic solvent containing small droplets of aqueous dye suspended in the bulk water phase. Stirring causes the oil phase to evaporate, leaving behind ink molecules encapsulated in polymer. Freeze drying in a lyophilizer removes any residual

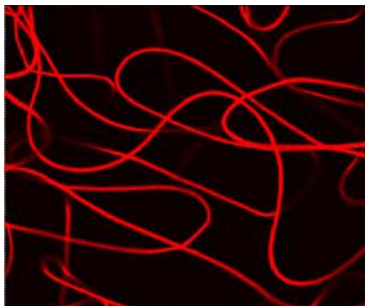


Figure 2: Encapsulated Rhodamine Core-Shell Fibers

water from the system, leaving small dye microspheres. The resultant microspheres can be suspended in deionized water, formulating our biostable ink.

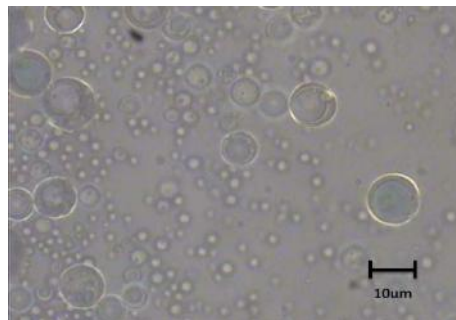


Figure 1: Encapsulated Blue Ink Microparticles

Another method of ink fabrication that we employed was the encapsulation of dye in biostable electrospun nanofibers, as shown in Figure 2. In order to test this, microfiber mats were electrospun from an emulsion that consists of PMMA, Rhodamine (an aqueous fluorescent compound), Span-80 (a nonionic surfactant), chloroform, dimethylformamide (DMF), and distilled water.³

We are going to utilize an ultrasound machine to destroy the PMMA surrounding the dye in order to allow release of the dye from our fibers and microparticles. Detection of dye release is possible from UV-visible light spectrophotometry of the water solution surrounding our samples after ultrasound treatment. We formulated standard curves for the dyes in water before encapsulation by correlating light absorption with known concentrations of dye. Ongoing studies include testing the viability of our ink in a porcine model as well as in the dermis of human skin surgically removed from plastic surgery patients.

¹ Harris Interactive, "One in Five U.S. Adults Now Has a Tattoo" *TheHarrisPoll*(2012)

² Kent, Kathryn, and Emmy Graber. "Laser Tattoo Removal: A Review." *Dermatologic Surgery: Official Publication for American Society for Dermatologic Surgery* 38.1 (2012): 1-5

³ Liao, Yiliang, Lifeng Zhang, Yi Gao, Zheng-Tao Zhu, and Hao Fong. "Preparation, characterization, and encapsulation/release studies of a composite nanofiber mat electrospun from an emulsion containing poly (lactic-co-glycolic acid)." *Polymer (Guildf)* 10 (2008): 1, 3, 5.

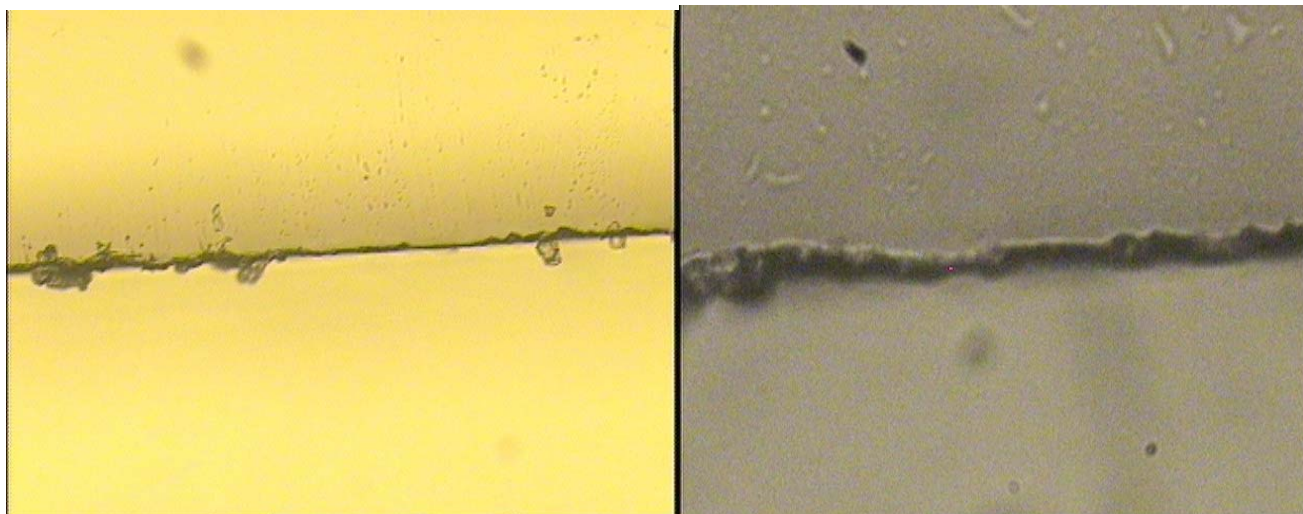
Synthesis of Larger Graphene sheets from Graphene Oxide using Ink-jet Printing

Tzadok Z. Hartman, Benjamin Goldman, Miriam Rafailovich

¹Rambam Mesivta, Lawrence, NY, ²Queens College, Flushing, NY, ³Stony Brook University, Stony Brook, NY

In 2004 a new allotrope of carbon was discovered: graphene. Graphene demonstrated amazing properties including being thermally conductive, electrically conductive, and harder than diamond. However, until recently there was no effective method to produce continuous sheets. The goal of this project is to effectively produce graphene sheets via ink-jet printing.

We first synthesized Graphene Oxide (GO) using a modified Hummer's¹ method. Then, after sonicating and centrifuging at 2500 rpm for 5 minutes, we dried the GO on slides. The dry GO was then suspended in 75:25 water:ethanol and a different sample was suspended in Flush©, and they were sonicated to break up the larger pieces. The suspension was then centrifuged to purify the GO. I then reduced the GO with 15mmol of NaBH₄ and stirred it with a magnetic stir bar. We then put the suspended graphene into an 80°C water bath in order to remove any remaining functional groups. The sample was then brought to Hilord Chemical Corp where we printed thin grids and lines onto Kapton.



Printed Graphene on Kapton under optical microscope: 100x objective (left) and 500x objective (right)

We successfully printed lines and a grid of graphene, but as of now have been unable to run the necessary tests in order to determine the specific properties of our samples. We must still do AFM and conductivity tests.

If the tests prove that this process works, the implications could be boundless. Computer speeds orders of magnitude greater than current designs, armor lighter and stronger than Kevlar and potential for room-temperature superconductors may all be within reach.

1 William S. Hummers Jr., Richard E. Offeman (March 1958) "Preparation of Graphitic Oxide"

Dermal Cells/Aging/Cancer/Adipocytes/Cell Migration/Fibrinogen

Chairs: Ariella Applebaum, Stern College for Women; Elianna Applebaum, Stern College for Women; Jason Kuan, Amherst College

Graduate Mentors: Sisi Qin

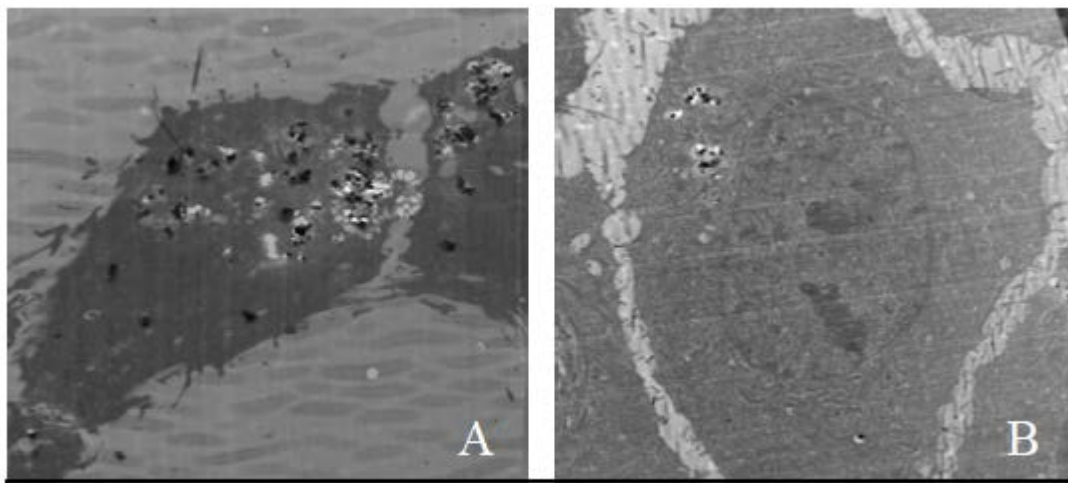


Figure 1: TiO₂ Anatase with DXM (A) and TiO₂ Anatase without DXM

The Proliferation and Differentiation of Dental Pulp Stem Cells on Graphene/P4VP Composite Substrates

Aaron Argyres Clayton High School, St. Louis, MO; **Mingu Kim** Hickman High School, Columbia, MO;

Yingjie Yu Department of Material Sciences and Engineering, Stony Brook University

Dr. Miriam Rafailovich Department of Material Sciences and Engineering, Stony Brook University

Dr. Marcia Simon School of Dental Medicine, Stony Brook University

There is a pressing need for new approaches of tissue engineering to replace the established method of bone grafted dental implants, due to various problems such as malformation and lack of grafting material. Stem cells are becoming a viable solution, as scientists become more capable of engineering specific environments for cell growth to induce proliferation and differentiation into desired cell lineages. Dental pulp stem cells (DPSC's) are mesenchymal stem cells extracted from the soft living tissue inside the tooth, an easily accessible location. DPSC's have a wide differentiation capability, with studies showing formation of stiffer tissues like dentin, odontoblasts, and cementoblasts, but also have the ability to form myocytes and neuronal cells that have the potential to repair muscle or brain tissues.¹

Proliferation and differentiation of stem cells is determined by three main principles: the type of stem cell, the underlying scaffold, and growth factors². We attempt to manipulate the morphology and surface chemistry to induce differentiation using P4VP/graphene composite thin films. Graphene is a carbon allotrope with remarkably high modulus and superconductivity. P4VP is a hydrophilic, biocompatible polymer shown in some cases to induce differentiation when patterned through electrospinning. Composite materials may have optimal morphology and surface chemistry, as well as being cost-efficient, as large graphene sheets are difficult to produce.

We attempted to engineer graphene/P4VP composite substrates with favorable physical and chemical properties in order to induce differentiation of DPSC's without traditional differentiation factors. Thin films of graphene/P4VP composites of concentrations 0.1%, 0.5%, 1%, 3%, 5%, and 10% along with 0.1%, 0.5%, 1% graphene oxide/P4VP composite, and pure P4VP were spin-coated onto silicon wafers. Cells were then plated and counted using standard procedure and a hemacytometer on days 3, 5, and 8 to check for cytotoxicity. For differentiation the cells were plated and grown for 28 days, with and without the differentiation factor dexamethasone.

AFM images revealed even distribution of graphene nanoplatelets on the P4VP polymer. Confocal microscopy displayed normally shaped cells as well as extensive cell growth at 8 days. Based on the graph (shown below), we propose that the P4VP and P4VP composites increased the standard rate of proliferation of the dental pulp stem cells. In the next few weeks, we will have confocal osteocalcin stain and electron microscopy images signifying the results of the differentiation study, the ultimate goal of our research. These results will determine the feasibility of P4VP/graphene composites for use in clinical dental and bone engineering.

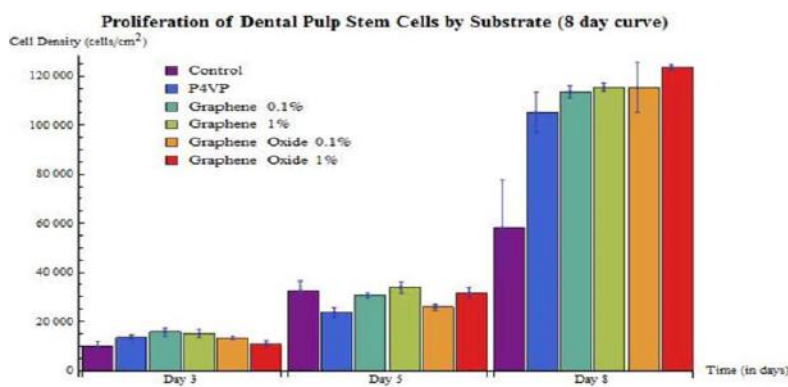


Figure 2: Proliferation Curve of Dental Pulp Stem Cells

¹Ito K. et al. (2011). Osteogenic Potential of Effective Bone Engineering Using Dental Pulp Stem Cells, Bone Marrow Stem Cells, and Periosteal Cells for Osseointegration of Dental Implants. *The International Journal of Oral & Maxillofacial Implants*, 26, 947-954.

²Reilly, et al. (2010). Intrinsic Extracellular Matrix Properties Regulate Stem Cell Differentiation. *Journal of Biomechanics*, 43, 55-62.

Influence of Hydrogel Substrate on Pseudorabies Virus Infection

Courtney Schwartz¹, Chantel Yang², Fan Yang³, Dr. Miriam Rafailovich³

¹The Wheatley School, Old Westbury, NY

²Commack High School, Commack, NY

³Dept. of Material Science and Engineering, Stony Brook University, Stony Brook, NY

Hydrogels are matrices of three-dimensional, hydrophilic polymeric molecules immersed in water. They display properties of both solid and liquid materials, and they are insoluble due to crosslinking. Crosslinking is a process in which one polymer is bonded to another polymer.¹ For this experiment, enzymatic cross-linking was used to create covalent bonds between the polymers. In terms of structure, hydrogels are very similar to the extracellular matrix of the tissue of many organs; thus, they are ideal scaffolds for studies pertaining to the dermis and penetration of the dermal layers.² In this investigation, hydrogels with varying stiffness and glucose levels were created as scaffolds to test virus infectivity on epithelial-like cells. Combined, hydrogel stiffness and glucose level can be used to mimic the conditions of the human body and skin at different stages of life because as humans age, the skin softens gradually. Conditions that cause blood sugar levels to be irregular, such as type 2 diabetes, also are more common as age increases. The goal of this project was to determine if conditions associated with aging can make an individual more prone to viral reproduction and infection.

In order to test the stiffness of hydrogels, five different concentrations of gelatin and microbial transglutaminase (mTG) hydrogels were created. Pre-warmed, sterilized gelatin, mTG, and glucose solution were mixed together via micropipettes. Four 6-well plates of gels were created, with one control (no hydrogel) and five concentrations as follows: 3:1, 15:1, 25:1, 75:1, 125:1 (gelatin:mTG). Each of the four plates contained 0, 30, 60, or 90 μ l of the glucose-buffer solution. Prior to cell plating, the hydrogels were tested using the rheometer for its elastic modulus. The elastic modulus is the tendency for a material to be deformed elastically.³ Afterwards, Dulbecco's Modified Eagle Medium and rabbit kidney 13 (RK13) cells were plated on the gels after a 24-hour incubation period. Pseudorabies virus (PrV) with a multiplicity of infection of 0.5 was then added to the wells and incubated for another 24 hours. RK13 cells were fixed with formaldehyde, an organic compound used to kill and preserve cells. Using Triton, which breaks the cell membrane and propidium iodide, a chemical that causes the RK13 cell nucleus to emit a red fluorescence and the viral nucleic acids to emit a green fluorescence, the infected RK13 cells were prepared for confocal microscopy.

Rheology results thus far indicate that our 3:1 hydrogels have higher elastic moduli than the 125:1 hydrogels. We plan to utilize confocal microscope images to calculate the percent of infection relative to the area covered by cells. Although this study does not involve human cells or pathogens, the results can provide information about viral infection in humans. Since PrV is a member of the herpesvirus family, it shares many characteristics with herpesviruses that infect human cells.⁴ Likewise, RK13 cells are mammalian cells, so they possess similarities to human cells. Therefore, results obtained from this study are likely to be similar to results that would be obtained in a study using human cells and pathogens. In order to expand on our research and make it more applicable to human life, we would like to substitute the PrV with HSV-1 and RK13 cells with dermal fibroblasts. Additionally, we would like to use a scaffold that can have adjustable porosity since aged skin also tends to be more porous.

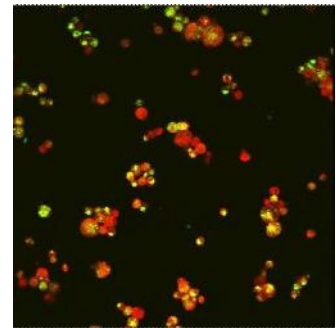


Figure 1 15:1 Hydrogel Confocal Microscope Image of PrV-Infected RK13 Cells

¹ Bhatnagar, D. (2012). *Influence of Deformable Substrates on Macroscopic and Microscopic Phenomenon of Tissue* (Unpublished doctoral dissertation). Stony Brook University, Stony Brook, NY.

² Drury, J. L., & Mooney, D. J. (2003). Hydrogels for tissue engineering: Scaffold design variables and applications. *Biomaterials*, 24, 4337-4351.

³ Gulrez, S. K. H., Al-Assaf, S., & Phillips, G. O. (2011). *Hydrogels: Methods of preparation, characterisation and applications*. Rijeka, Croatia: InTech.

⁴ Roizman, B. (Ed.). (1983). *The herpesviruses*, vol. 2 (Vol. 2). New York, NY: Plenum Press.

The Effect of Dermal Fibroblast Age on cell Migration Rates on Electrospun Scaffolds for Wound Healing

Christina Chen, Diamond Bar High School, Diamond Bar, CA

Kevin Liu, Interlake High School, WA

Sisi Qin, Stony Brook University, Stony Brook, NY

Jason Kuan, Amherst College, MA

Miriam Rafailovich, Stony Brook University, Stony Brook, NY

The study of skin tissue rejuvenation is vastly important for wound victims such as burn patients and those affected by ulcers or skin cancer. Scientists have struggled to find a way to perfectly regenerate skin tissue in adults therefore, the goal of our research is to investigate the effect of age and the effect of electrospun fibers on the migration rate of dermal fibroblast migration rates. A faster cell migration rate would result in a better healing rate; therefore, if there is a substantial difference in the movement of older HDF and younger HDF, this would prove that adult cells tend to lose their ability to migrate over time [Krawczyk]

First, we prepared the surfaces on which the dermal fibroblasts will be cultured on. To do so, two solutions were made: Solution 1 consisted of 30mg/mL Polymethyl methacrylate (PMMA) in 10mL of Toluene and Solution 2 consisted of 20% PMMA in weight dissolved in 3.2g of Chloroform. Next, we spun cast Solution 1 onto 60 glass cover slips and 50 glass coverslips were spin casted with the same Solution 1 but were not electrospun with PMMA fibers in order to provide a control. After spin casting, the first 60 glass coverslips were taped onto a sheet of aluminum foil using double sided tape. Using a kd Scientific electrospinner, powered by a Powerstat Variable Autotransformer, the aluminum foil was taped on to the collector, spun for 2 minutes and finally annealed at 120°C. Next, we defrosted young dermal fibroblast cells from a Caucasian Female of 31 years (CF31) and old dermal fibroblasts acquired commercially from an 84-87 year man (AG11-744). These cells were then plated on the electrospun glass coverslips and the thin film coverslips. The last step was to measure the speed at which the cells were traveling on these scaffolds using an optical microscope. Pictures of the cells were taken every 15 minutes for four days.

As shown in Fig. 1, by the fourth day, old fibroblast cells migrating on spin casted scaffolds moved at an average rate of 53.39 $\mu\text{m}/\text{day}$ [with an error of 1.91 standard deviations], old cells on thin films migrated at 54.14 $\mu\text{m}/\text{day}$ [error of 1.40 standard deviations], young cells on spin casted scaffolds at 38.47 $\mu\text{m}/\text{day}$ [error of 1.36 S.D], and finally young fibroblast cells on thin films moved at a rate of 52.18 $\mu\text{m}/\text{day}$ [3.18 S.D]. With this data, we are unable to confidently assume that fibers had a substantial effect on cell migration rates, however, surprisingly, the AG11-744 cells traveled at a much faster rate than the CF31 cells. We presume that this might be due to the number of passages each strain of cells has been exposed to. At the beginning of the experiment, the CF31 cells were on their 11th passage while the AG11-744 cells were only on their 1st passage. If this experiment were to be continued, a possible step would be to minimize the variables that would alter the accuracy in data.

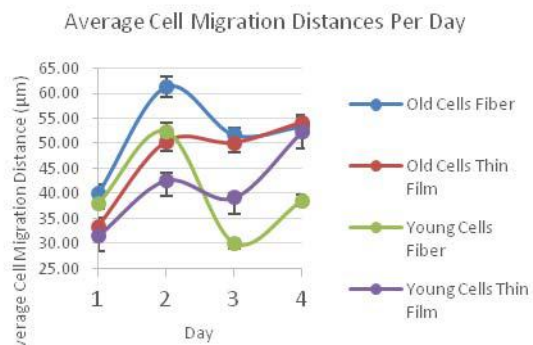


Fig. 1: Graph detailing migration distances

Analysis of the migration and traction forces of dermal fibroblasts on hydrogel surfaces of varying stiffness

Jason Zarate, Sachem High School East, Farmingville, NY

Ruth Kopyto, Stella K. Abraham High School for Girls, Hewlett, NY

Jason Kuan, Amherst College, Amherst, MA

Sisi Qin, Department of Materials Science and Engineering, Stony Brook University, Stony Brook, NY

Dr. Miriam Rafailovich, Department of Materials Science and Engineering, Stony Brook University, Stony Brook, NY

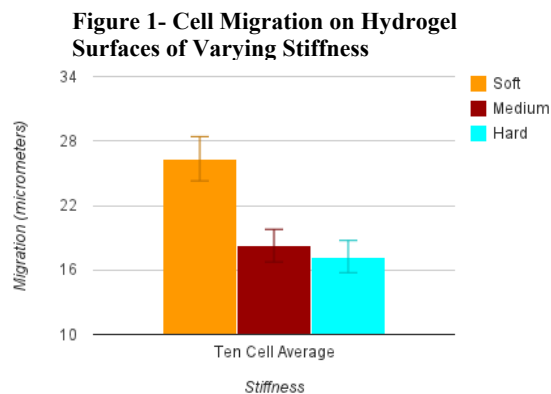
Dr. Marcia Simon, Dental School, Stony Brook University, Stony Brook, NY

The rate of healing in wounded patients is, and will continue to be, a prevalent medical issue. Wound healing, which involves tissue repair by cells near the wound, is influenced by how well fibroblasts can migrate and form an ECM (extracellular matrix) with components including collagen and fibronectin (Midwood, Williams & Schwarzbauer, 2004). The mechanics of the traction forces exerted by fibroblasts during their “pulsed” migration are well known (Pan, Ghosh, Liu, Clark & Rafailovich, 2009). What is not known is the effect of the migration surface on the rate of migration and the magnitude of traction forces. The purpose of this project is to study the effect of varying stiffness of biologically relevant hydrogel surfaces on the rate of migration and traction forces of dermal fibroblasts.

Six hydrogels were made in six separate 35 mm diameter wells with two of each stiffness (soft, medium, and hard). Soft gels (MTG to gelatin ratio of 1:125), medium gels (1:25 ratio) and hard gels (1:3 ratio) were created. Fluorescent dermal fibroblasts taken from a patient in her low thirties were cultured and placed on the gels with a .3% concentration of 1 μm fluorescent beads. The cells' actions, after detachment as a result of exposure to trypsin, and fluorescent bead displacement were recorded using confocal microscopy. The displacement of the beads on the hydrogel can be analyzed using the DISC technique which allows for the measurement of fibroblast traction forces. For cell migration analysis, gels were also created on a 24 well plate with the same ratios of MTG to gelatin, but without fluorescent beads. Nonfluorescent CF31 dermal fibroblasts were placed on the gels. The movement of the cells was measured using MetaMorph software.

The cell migration data collected shows that migration was greater as the stiffness of the gel decreased. Cells migrated on the softest gel at an average of 26.35 μm compared to 18.27 μm and 17.25 μm on the medium and hard gels, respectively (see Figure 1). DISC technique has not been used on confocal images of fluorescent bead displacement to measure traction forces yet.

These results indicate that a softer migration surface might assist in the ability of fibroblasts to move to an area that requires tissue repair. This is somewhat useful in the medical world as the creation of a biomimetic surface to promote increased fibroblast migration and more efficient tissue repair at the site of wounds is possible. To further this research, studies must be done on other biologically relevant migration surfaces as well as more trials using different ages and types of fibroblasts.



Midwood, K. S., Williams, L. V., & Schwarzbauer, J. E. (2004). Tissue repair and the dynamics of the extracellular matrix. *The International Journal of Biochemistry and Cell Biology*, 36(6), 1031-1037.

Pan, Z., Ghosh, K., Liu, Y., Clark, R. A. F., & Rafailovich, M. (2009). Traction stresses and translational distortion of the nucleus during fibroblast migration on a physiologically relevant ecm mimic. *Biophysical Journal*, 96, 4286-4298

The Effect of Titanium Dioxide Nanoparticle Exposure on Cellular Migration, Proliferation, Morphology, and Collagen Contraction in Adipose-Derived Stem Cells

¹Nicolette Almer, ¹Kimia Ziadkhanpour,

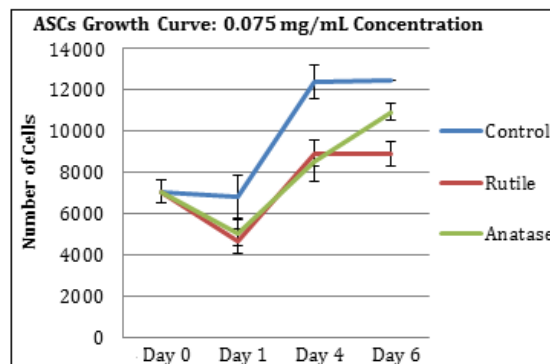
²Tatsiana Mironava, ²Miriam Rafailovich, ³Marcia Simon

¹Plainview – Old Bethpage John F. Kennedy High School, Plainview, NY, ²Department of Materials Science and Engineering, State University of New York at Stony Brook, Stony Brook, NY, ³Department of Oral Biology and Pathology, School of Dental Medicine, State University of New York at Stony Brook, Stony Brook, NY

Nanotechnology has become a dynamic scientific field of research, leading to developments in cancer therapy, antibody targeting, and manufacturing. However, the use of nanotechnology in consumer products has proven to be a polemic issue, arousing concerns regarding long-term environmental and health safety. Prior studies have shown that the inherently small size of nanoparticles increases the likelihood of cellular uptake, leading researchers to believe that these particles can affect organisms at the cellular level.¹

In this experiment, the effect of titanium dioxide (TiO₂) nanoparticle exposure on cellular functions, mechanisms, and protein production was determined using adipose-derived stem cells (ASCs) as a model. Since TiO₂ nanoparticles are commonly used as whitening pigments in sunscreens and cosmetic creams, there is significant potential for TiO₂ nanoparticles to pass through the successive layers of the skin (up to the subcutaneous layer, where ASCs are stored), penetrate cells, and affect their normal functioning.^{1,2}

ASCs underwent a number of tests, including those for cell migration, collagen contraction, particle penetration using Transmission Electromicroscopy (TEM), and for production of the adiponectin protein using enzyme-linked immunosorbent assay (ELISA). A growth curve was created to track ASC growth over a 6-day period. Samples were cultured separately with anatase and rutile (crystalline forms of TiO₂) at concentrations of 0.075 mg/mL, 0.05 mg/mL, and 0.10 mg/mL, and counted using standard hemacytometer procedure. Cells were split from a flask and plated separately for the experiments involving cell migration, collagen contraction, TEM, and ELISA.



Results indicated that cells proliferated best when treated with 0.075 mg/mL TiO₂ nanoparticles. The greatest number of cells (10,933) was found in the sample treated with 0.075 mg/mL anatase, an interesting result considering that in most studies, anatase is more detrimental to cell growth than rutile is. As expected, the least number of cells on average (9,000 for rutile, 8,533 for anatase) grew when treated with 0.10 mg/mL, the highest concentration of TiO₂ used in this experiment.

In the future, we intend to observe the ASC samples using TEM and determine the extent of adiponectin production using ELISA. An additional course of study would involve examination of the effect of gold or zinc nanoparticles (AuNPs and ZnNPs) on the cellular functioning of ASCs to highlight how different nanoparticle treatments affect these cells. Results from these experiments will help the scientific community further grasp the health-related effects of nanotechnology on humans.

¹Li, Shi-Qiang, Rong-Rong Zhu, Hong Zhu, Meng Xue, Xiao-Yu Sun, Si-De Yao, and Shi-Long Wang. "Nanotoxicity of TiO₂ Nanoparticles to Erythrocyte in Vitro." *Food and Chemical Toxicology* 46.12 (2008): 3626-631.

²Pan, Zhi, Wilson Lee, Lenny Slutsky, Richard A. F. Clark, Nadine Pernodet, and Miriam H. Rafailovich. "Adverse Effects of Titanium Dioxide Nanoparticles on Human Dermal Fibroblasts and How to Protect Cells." *Small* 5.4 (2009): 511-20.

Controlling Anti-Thrombogenic Properties of Polymer Surfaces Through Sterilization Techniques for the Development of Safer Medical Device Implantation

Paige Botie¹, Yaakov Eiferman², Luidi Zhang³, Miriam H. Rafailovich³, Dennis Galanakis⁴, Marcia Simon⁵

¹Half Hollow Hills High School West, Dix Hills, NY, ²Rambam Mestiva High School, Lawrence, NY, ³Department of Materials Science and Engineering, ⁴Department of Pathology, ⁵Department of Oral Biology and Pathology at Stony Brook University.

Fibrinogen is an essential blood protein that plays an important role in the coagulation cascade, as well as being the major determinant of blood viscosity and blood flow. Coagulation is essential in wound healing, but it can also be detrimental in surgical circumstances, concerning the implantation of stents or implants. Uncontrolled thrombogenesis on such medical devices can lead to the obstruction of the blood in the circulatory system. The goal of this research is investigate the properties of different polymers, and the effect of UV ozone sterilization treatments of these polymers, as well as study their interaction with normal fibrinogen and des- α C fibrinogen and endothelial cells (HUVEC) to help prevent unwanted thrombogenesis resulting from the insertion of medical devices.

20 mg/mL Polystyrene (PS), a polymer commonly used in medical devices, was spin coated onto silicon wafers. HUVEC cells were then plated onto bare PS, PS with 4 mg/mL normal fibrinogen (Fb), and PS with 4 mg/mL des- α C Fb and observed at a 24h and 48h time point. From previous research, it is known that fibrinogen fibers will form on the PS surface due to the surface chemistry; it is hydrophobic.¹ Therefore, the PS with the absence of Fb served as the experimental control. An additional sample of PS coated silicon wafers was treated with a plasma UV ozone sterilization technique. We hypothesized that sterilizing the PS would alter the surface chemistry of the PS and discourage the formation of fibers. 7 mg/mL Poly(4-vinyl pyrimidine) (P4VP), a hydrophilic polymer, was spin coated onto Si wafers and HUVEC cells were plated on bare P4VP, P4VP with 4 mg/mL normal Fg, and 4 mg/mL des- α C Fb. Fb was placed onto the Si wafers with different polymer surfaces to investigate hydrophobic surface-induced Fb aggregation. Using the atomic force microscope (AFM), we examined fibers that formed without the presence of thrombin (Figure 1). Further tests were conducted to analyze whether damaged Fb lacking the intact α C region will be able to develop fibers. Contact angle analysis was conducted to determine the hydrophilicities of the PS surface, PS UV ozone sterilized surface, and the P4VP surface. The hydrophilicities of a surface is a factor in whether the surface can support fiber formation. A hydrophobic surface exposes the α C domains and other cryptic functional sites of Fb molecules, allowing lateral aggregation to occur and causing the production of fibers. Upon contact angle analysis, the bare PS was found to have the greatest contact angle (92.136 $\text{\textcircled{left}}$, 92.003 $\text{\textcircled{right}}$) and the P4VP is was found to have a smaller average contact angle (61.613 $\text{\textcircled{left}}$, 62.903 $\text{\textcircled{right}}$). For the sterilization process to discourage fiber formation in medical devices the surface must be made more hydrophilic. Upon analysis, the PS treated with UV ozone sterilization was found to have the smallest average contact angle (50.5225 $\text{\textcircled{left}}$, 50.8175 $\text{\textcircled{right}}$). This is significant because this sterilization process can modify the PS, the most commonly used polymer in medical devices, to prevent large fiber formation and decrease risks associated with implanting such medical devices. Confocal microscopy analysis and further AFM analysis will be conducted to determine the action of the HUVEC on the different surfaces and details on the fiber formation on these surfaces.

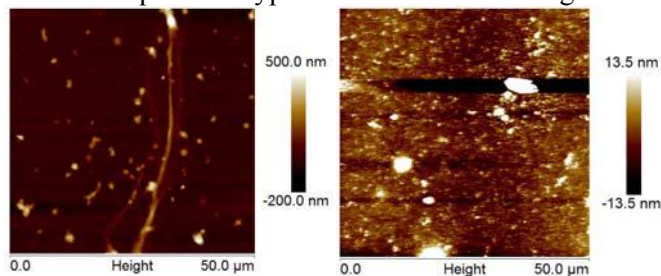


Figure 1: Fb on the bare PS surface exhibited defined fiber formation while the UV sterilized PS surface exhibited globular aggregates.

Further tests were conducted to analyze whether damaged Fb lacking the intact α C region will be able to develop fibers. Contact angle analysis was conducted to determine the hydrophilicities of the PS surface, PS UV ozone sterilized surface, and the P4VP surface. The hydrophilicities of a surface is a factor in whether the surface can support fiber formation. A hydrophobic surface exposes the α C domains and other cryptic functional sites of Fb molecules, allowing lateral aggregation to occur and causing the production of fibers. Upon contact angle analysis, the bare PS was found to have the greatest contact angle (92.136 $\text{\textcircled{left}}$, 92.003 $\text{\textcircled{right}}$) and the P4VP is was found to have a smaller average contact angle (61.613 $\text{\textcircled{left}}$, 62.903 $\text{\textcircled{right}}$). For the sterilization process to discourage fiber formation in medical devices the surface must be made more hydrophilic. Upon analysis, the PS treated with UV ozone sterilization was found to have the smallest average contact angle (50.5225 $\text{\textcircled{left}}$, 50.8175 $\text{\textcircled{right}}$). This is significant because this sterilization process can modify the PS, the most commonly used polymer in medical devices, to prevent large fiber formation and decrease risks associated with implanting such medical devices. Confocal microscopy analysis and further AFM analysis will be conducted to determine the action of the HUVEC on the different surfaces and details on the fiber formation on these surfaces.

¹Koo, J et al. "Control of Anti-Thrombogenic Properties: Surface-Induced Self-Assembly of Fibrinogen Fibers." *Biomacromolecules*. (13) 1259-1268 (2012).

The Adverse Effects of Titanium Dioxide and Zinc Oxide Nanoparticle on Human Cervical Adenocarcinoma (HeLa) Cell Membranes and Ion Current Flow

Shoshana Guterman¹, Emma Zawacki², Eliana Applebaum³, Ariella Applebaum³, Yichen Guo⁴, Dr. Miriam Rafailovich⁴, Dr. Tatsiana Miranova⁴, Dr. Peter Brink⁴, Dr. HZ Wang⁴, and Dr. Chris Gordon⁴

¹Yeshiva University High School for Girls, Hollis, NY; ²Smithtown High School East, St. James, NY; ³Stern College for Women, New York, NY; ⁴SUNY Stony Brook University, Stony Brook, NY

Nanoparticles are ubiquitous in one's daily lives; they are widely used as active ingredients in cosmetics, sunscreens, toothpastes, paints and numerous other materials that we encounter habitually (Nel, et. al.). Titanium Dioxide (TiO₂), in both its rutile and anatase forms, and Zinc Oxide (ZnO) are commonly found in such household goods; however, these particles are also known to have devastating effects on human cells with anatase and zinc particles being the cause of greater damage (Pan, et. al.). In this study, human cervical adenocarcinoma (HeLa) cells were cultured to study the cytotoxic effects of ZnO and TiO₂ nanoparticles and to investigate their damaging effects on cell membranes, specifically on ion current flow. To observe this damage, several methods of experimentation including the patch clamp apparatus, thermal gravimetric analysis (TGA), and transmission electron microscopy (TEM) were utilized. To begin, HeLa parental cells were plated, and after 24 hours the synthetic glucocorticoid steroid, dexamethasone (DXM) was added. DXM is thought to increase the stiffness of the membrane and to prevent nanoparticle penetration; therefore it was added to plated cells to see if it could provide further protection to the HeLa cells (Chen, et. al.). 24 hours later, nanoparticles were added to the cells resulting in samples with various nanoparticle concentrations: 0.1 mg/mL anatase, 0.15 mg/mL anatase, 0.2 mg/mL anatase, 0.1 mg/mL rutile, 0.15 mg/mL rutile, 0.2 mg/mL rutile, and 0.01 mg/mL zinc. After conducting numerous patch-clamping experiments, the capacitance, current, electric potential, and negative pressure required to patch were observed. The capacitance is proportional to the cell size allowing us to determine if the membrane current is a result of nanoparticles opening pre-existing channels or recruiting new channels. It was found that the DXM-ZnO had the highest current, 2.03 pA, when patching; higher than that of both DXM-TiO₂ rutile, 1.52 pA and anatase, 1.09 pA. Additionally, the TGA was used to burn all organic matter of the sample, leaving only a measurable concentration of nanoparticles within the cell. It was discovered that anatase TiO₂ had the highest cellular concentration, with the addition of DXM reducing nanoparticle uptake. Finally, the cells were observed using TEM and discovered that a higher concentration of nanoparticles was present in the cell untreated with dexamethasone, making it apparent that DXM prevented some nanoparticle uptake (Figure 1). Although the toxicity of nanoparticles is apparent from these results, we plan on using flow cytometry to record how many cells have nanoparticles (Pan, et. al.). Additionally, with the inclusion of bafilomycin, an inhibitor of endocytosis, TEM images of the cells will be observed to see if the nanoparticles are entering the membrane either through endocytosis or permeating the membrane. In conclusion, this study shows that both TiO₂ and ZnO have cytotoxic effects on HeLa cells; however, such effects appear to be inhibited through the addition of DXM.

Nel, A. et. al. "Toxic Potential of Materials at the Nanolevel" *Science* (2006) 311 622-627

Pan, Zhi et. al. "Adverse Effects of Titanium Dioxide Nanoparticles on Human Dermal Fibroblasts and How to Protect Cells" *Small* (2009) 5 511-520

Chen, Yu-Xia. et. al. "Dexamethasone enhances cell resistance to chemotherapy by increasing adhesion to extracellular matrix in human ovarian cancer cells" *Endocrine-Related Cancer* (2010) 17 39-50

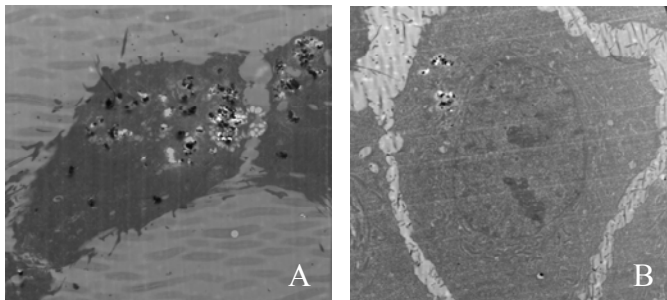


Figure 1: TiO₂ Anatase with DXM (A) and TiO₂ Anatase without DXM

Drug Delivery and Disease Detection

Chairs: Jacob Wax, University of Pennsylvania;
Tom Van Bell, The Wheatley School;

Graduate Mentor: Vianney Delplace, Institut
Galien University of Paris

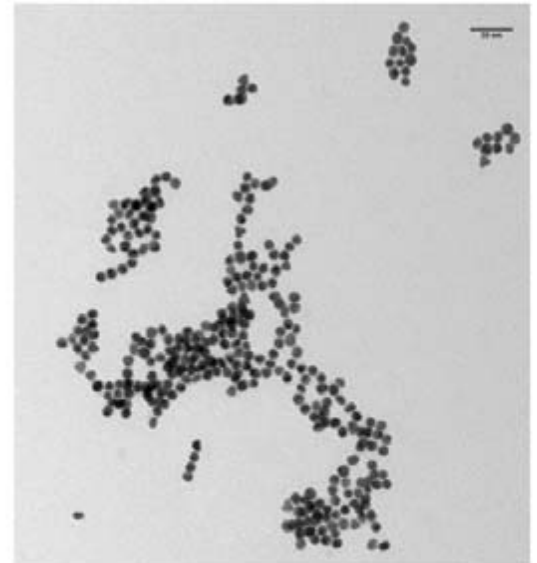
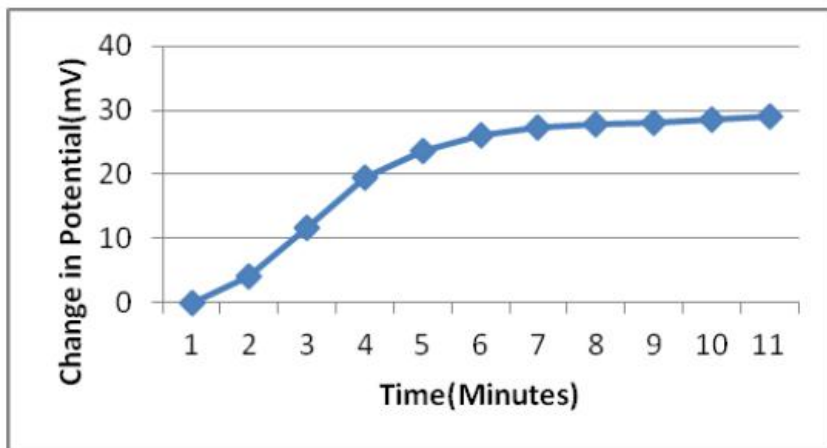


Figure 2
TEM Image of AuNPs

Functionalization of Gold Nanoparticles as Drug Delivery Agents for Treatment of Cryptococcosis

Allison Chowdhury, Greta Huang, Vianney Delplace, Miriam Rafailovich
The Wheatley School, Commack High School, Stony Brook University

Cryptococcosis has become an increasingly prevalent disease in today's global community. Caused by the human fungal pathogens *Cryptococcus neoformans*, contraction results in fatal infections of the central nervous system (Voelz, K., Johnston S., Rutherford, J. & May, R. C., 2010). The Centers for Disease Control estimate over 1 million new cases of cryptococcosis annually, with mortality of 650,000 deaths per annum (Del Poeta, M. & Casadevall, A., 2011). BHBM is implicated in treatment of cryptococcosis, through inhibition of glucosylceramide synthesis in fungi.

Recently, gold nanoparticles (AuNPs) have demonstrated potential in drug delivery applications because of their essentially non-toxic and photo-adaptable properties (Conde, J., Doria, G. & Baptista, P., 2012) [Figure 1]. The most stable of all known metal nanoparticles, AuNPs are easily functionalized with thiol because of the strong Au-S bond. Thiolated AuNPs can be further adapted to include various functional groups for delivery and imaging modalities.

The purpose of this study was to synthesize functionalized AuNPs for BHBM drug delivery and investigate its effectiveness in the treatment of Cryptococcosis infected murine macrophages. AuNPs were synthesized using the Turkevich method and grafted onto 6-Mercaptohexanoic acid containing a thiol group conjugated to BHBM. The ideal thiol concentration for grafting was determined to be between .5 and 1 μ l. Nanoparticles were characterized with Transmission Electron Microscopy [Figure 2] and UV-Visible spectroscopy. Average AuNP size was determined to be ~11 nm.

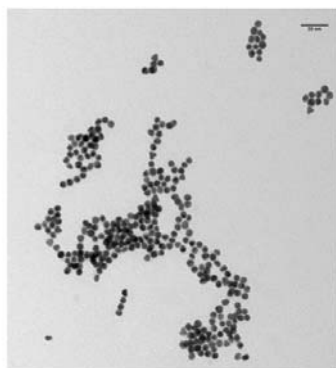


Figure 2
TEM Image of AuNPs

Drug conjugation was confirmed via Nuclear Magnetic Resonance spectroscopy. J774 macrophages were infected with *Cryptococcus neoformans* and exposed to AuNPs with and without BHBM.

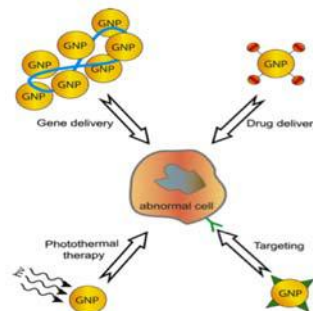


Figure 1
Various AuNP applications
Ghosh et al.

Voelz, K., Johnston S.A., Rutherford, J. C., May, R. C. (2010) Automated Analysis of Cryptococcal Macrophage Parasitism Using GFP-Tagged Cryptococci, *PLoS ONE* 5(12).

Del Poeta, M. & Casadevall, A. (2011). Ten Challenges on Cryptococcus and Cryptococcosis. *Mycopathologia*, 173, 303-310.

Conde, J., Doria, G. & Baptista, P. (2012) Noble Metal Nanoparticles Applications in Cancer. *Journal of Drug Delivery*, 2012, 1-12.

Creation and Optimization of a Potentiometric Biosensor for the Detection of Damaged Fibrinogen Molecules

Benjamin Khakshoor North Shore Hebrew Academy High School, Great Neck, NY

Jacob Wax University of Pennsylvania, Philadelphia, PA

Daniela Czemerenski Yale University, New Haven, CT

Vianney Delplace Institut Galien University of Paris-Sud

Yingjie Yu, Kuanche Feng Department of Material Sciences and Engineering Stony Brook University, Stony Brook, NY

Miriam Rafailovich Department of Material Sciences and Engineering Stony Brook University, Stony Brook, NY

Biosensors are widely used today to detect and diagnose patients with various medical conditions, one of which being damaged fibrinogen. Fibrinogen plays a key role in coagulation and inflammation; individuals who suffer from damaged fibrinogen have an impaired ability to form thromboses, or blood clots. Irregular fibrinogen structures are associated with cardiovascular disease, liver damage, thrombosis, and bleeding disorders¹. A potentiometric biosensor can detect damaged fibrinogen molecules through molecular imprinting; the biosensor uses biological signals to relay electrical signals that can be measured using a potentiometer².

In this study, we imprinted fibrinogen molecules on a 2.0cm by 0.5cm gold plated silicon wafer. To imprint the molecules we placed the gold wafer in an incubation solution consisting of 0.2mg thiol, 0.5mL DMSO, 0.05mg fibrinogen, and 9.5mL DPBS. During this process, a self-assembled monolayer of thiol forms on the surface of the wafer; the fibrinogen molecules leave imprints on the wafer, creating complimentary cavities. After incubation, the molecules are washed off with DI water, leaving just the monolayer of thiol and imprints of the fibrinogen molecules. We then submerge the wafer in a solution of DPBS and measure the potential voltage of the wafer. When the imprinted molecules are reintroduced into the system, the potential voltage reacts to the imprinted molecules—we can measure this with a potentiometer. As seen in Figure 1, we observed a significant voltage change of 27mV, indicating the presence of the biomarker in the test solution.

It is imperative to optimize the biosensor for clinical use. In this study, we optimized the efficiency and accuracy of the device by testing different concentrations and incubation times.

In the future, we plan to cross test the imprinted fibrinogen wafers with damaged fibrinogen and hemoglobin. We will also imprint different damaged fibrinogen to see if we can detect certain types of damaged fibrinogen. Using this method, we can test to see if a patient has damaged fibrinogen and test to see which type of damaged fibrinogen the patient has.

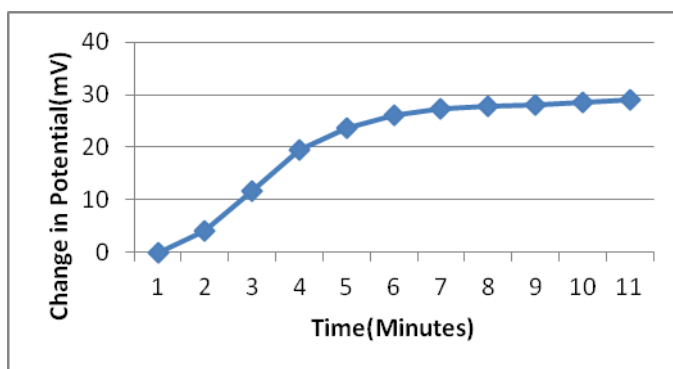


Figure 1: Fibrinogen Detection

¹ Koo, Jaseung, et al. "Evaluation of Fb Self-assembly: Role of its α C Region." *NIH Public Access* 8(12): 2727–2735 (2011). NIH. Web. 03 Aug. 2012.

² Wang, Yantian, et al. "A Potentiometric Protein Sensor Built with Surface Molecular Imprinting Method." *Biosensors and Bioelectronics* 24.1 (2008): 162-66. Print.

The Effects of PLGA Nanoparticles and Surfactant on Endothelial Cell Cytotoxicity and Angiogenesis

Daphne Chen, Palm Harbor University High School, Palm Harbor, FL

Leandra Meraglia-Garcia, St. Anthony's High School, South Huntington, NY

Vianney Delplace, Institut Galien, Universite-ParisSud, Paris, France

Dr. Marcia Simon, Oral Biology and Pathology, Stony Brook University, Stony Brook, NY

Dr. Miriam Rafailovich, Dept. of Materials Science and Engineering, Stony Brook University, Stony Brook, NY

Nanoparticles (particles <100 nm diameter) present medical dangers due to their high surface-to-volume ratio, which makes the particles highly reactive. Poly(lactide-co-glycolide) (PLGA) contains two monomers that are easily metabolized by the body during the Krebs cycle, therefore a minimal systemic toxicity is associated with the use of PLGA for drug delivery or biomaterial applications. PLGA is approved by the U.S. FDA and European Medicine Agency (EMA) in various drug delivery systems for humans². We will study the cytotoxicological effects and angiogenesis assay using a surfactant with a negative charge (Pluronic-68 [PF68, -]) on endothelial cells. Angiogenesis is the growth of new blood vessels from pre-existing blood vessels. It is a natural, vital biological process, but it is also a sign of a tumor's transition from benign to malignant. In this way, the project has biomedical applications to cancer patients in need of specialized drug delivery. The goal of this project is to determine whether a negatively charged surfactant on the nanoparticles will aid or hinder cell proliferation as well as endothelial cell angiogenesis.

The protocol we used to create nanoparticles came from the Laboratoire de Physico-Chimie. Our organic solvent was ethyl acetate. We mixed our organic solvent with 100mg of PLGA, followed by vortexing until the solutes were completely dissolved. This resulted in a homogenous solution that would mix with another solution of the desired surfactant plus deionized water. After combining our solutions we vortexed again and used a sonicator to achieve a consistent blend, which was vigorously stirred on a magnetic stir plate for 4 hours in order for the organic phase to evaporate¹. Afterwards, centrifugation of the 20-50 mL solution yielded a dense pellet of nanoparticles, which we suspended in deionized water, dried using a lyophilizer, and placed in media for use in the experiment. Concerning the biological aspect of our project, two 24-well plates and one 6-well plate worth of endothelial cells will be plated in order to feed with data collected 24 hours and 48 hours after exposure. The nanoparticle concentrations tested will be 0.1mg/mL and 0.4mg/mL. Tests run during the experiment will include a toxicity test as well as a test to see the nanoparticles' effects on the angiogenesis process. We will cell count at the two determined time points to ascertain whether the cells were killed or proliferated at a normal or accelerated rate, and observe the angiogenesis assay.

If the work in our project yields beneficial results, capillary blood vessel formation could be efficiently manipulated. This would help many doctors who treat debilitating conditions, including cancer and skin diseases. The future research for our project would include making additional nanoparticles for rerunning tests on the endothelial cells as well as experimenting with additional surfactants. This would determine more accurate and substantial results.

[1] Mura, S., Hillaireau, H., Nicolas, Kerdine-Römer, S., Le Droumaguet, B., Deloménie, C., Nicolas, V., Pallardy, M., Tsapis, N., & Fattal E. (2011, October). Biodegradable nanoparticles meet the bronchial airway barrier: How surface properties affect their interaction with mucus and epithelial cells. *BioMacromolecules*, 2 (11), 4136-4143. DOI: 10.1021/bm201226x.

[2] Danhier, F., Ansorena, E., Silva, J., Coco, R., Le Breton, A., & Préat, V. (2012). Plga-based nanoparticles: An overview of biomedical applications. *Journal of Controlled Release*, 161(2), 505-522. <http://dx.doi.org/10.1016/j.jconrel.2012.01.043>.

Treating *Cryptococcus* Infections by Use of PLGA Nanoparticles Loaded with Novel Antifungal Drug BHBM

Luke Chen¹, Siavash Parkhideh², Vivek Subramaniam³

Thomas Van Bell⁴, Dr. Amir Farnoud⁵, Yan Xu⁶, Dr. Visesto Mor⁵, Dr. Maurizio Del Poeta⁵, Vianney Delplace⁷, Dr. Miriam Rafailovich⁶

¹ Blue Valley High School, Stilwell, KS, ² Ward Melville High School, East Setauket, NY, ³ Westborough High School, Westborough, MA, ⁴ The Wheatley School, Old Westbury, NY, ⁵ Department of Biochemistry & Cell Biology, SUNY, Stony Brook, NY, ⁶ Department of Materials Science and Engineering, SUNY, Stony Brook, NY, ⁷ Institut Galien Paris-Sud, UMR CNRS 8612, Univ Paris-Sud, Faculté de Pharmacie

Traces of the fungus *Cryptococcus* can be found in the bodies of almost every human, but for immunocompromised patients, mainly people suffering from HIV/AIDS, it can cause fatal meningoencephalitis. To create a more specific approach to target *Cryptococcus*, we chose to encapsulate the novel antifungal agent BHBM in poly(lactic-co-glycolic acid) (PLGA) nanoparticles. PLGA was chosen because it is an FDA approved biomaterial and has superior biodegradable and biocompatible properties. To be attracted to the negatively charged fungus, the PLGA nanoparticles were coated with the positively charged surfactant, specifically chitosan chloride (CS). Our goal is to use this method to provide us with an effective means of targeting *Cryptococcus* to prevent fungal-related deaths in immunocompromised patients.

PLGA nanoparticles were synthesized by the emulsion evaporation technique. The desired polymer was dissolved into an organic phase (dichloromethane and acetone in a 1:1 v/v ratio), and emulsified with a surfactant in a water phase (CS and PVA). Then, the two phases were mixed, vortexed, sonicated with a Misonix Sonicator 3000, and finally magnetically stirred to evaporate away the organic solvents. The remaining suspension was then centrifuged to isolate the nanoparticles. (Mura 2011) The nanoparticles were tested for toxicity on cells, using the immortalized cell line J774A.1 (murine macrophages). Some J774A.1 cells were exposed to *Cryptococcus neoformans* and treated with PLGA/CS nanoparticles containing BHBM at a concentration of 20 mg/mL while other infected cells were treated with unloaded PLGA/CS nanoparticles.

The drug encapsulation efficiency of BHBM was measured through testing with the Thermo Scientific Evolution 220 UV-Visible Spectrophotometer. Known concentrations of BHBM in chloroform were made and measured (Figure 1) to elicit a standard curve for absorption vs. concentration.

For future studies, we would like to determine the distribution of nanoparticle size, via dynamic light scattering (DLS). We also plan to use high-performance liquid chromatography (HPLC) to more accurately determine encapsulation efficiency. Additional studies will be done on using other biodegradable and biocompatible polymer nanoparticles to encapsulate BHBM to improve encapsulation efficiency and release profile.

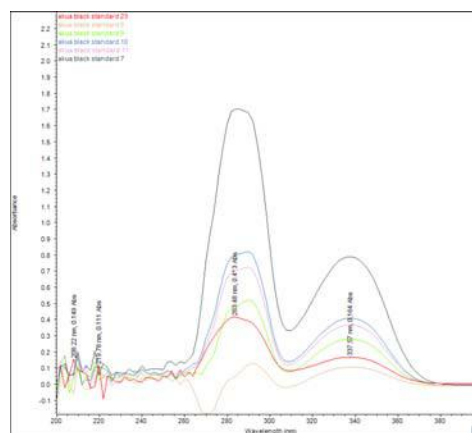


Figure 1: BHBM UV Vis Curve for Varying Concentrations

Citations:

Mura S, Hillaireau H, Nicolas J, et al. Influence of surface charge on the potential toxicity of PLGA nanoparticles towards Calu-3 cells. Int J Nanomedicine. 2011;6:2591-605.

The Effects of Ultraviolet-B Exposure and Rutile Titanium Dioxide Nanoparticles on *Cryptococcus*-infected Macrophage Cells

Matthew Kempster¹ in conjunction with Vianney Delplace², Yan Xu², Maurizio Del Poeta², Amir Farnoud², Tatsiana Mironava² and Miriam Rafailovich²

¹Mira Loma High School, Sacramento, CA, USA

²Stony Brook University, Stony Brook, NY, USA

Cryptococcosis is a potentially fatal disease caused by two species of fungi in the genus *Cryptococcus*. The motivation for an effective treatment for cryptococcosis is overwhelming; to date, it is known to cause meningitis, antigenemia, and pneumonia. The adverse effects of *Cryptococcus* spp. are non-discriminative; *C. neoformans* primarily ails immunocompromised humans by lodging in alveoli, as seen in Figure 1, whereas *C. gattii* can kill even immunocompetent humans. As such, a great deal of research is being conducted to solve this problem. Existing anticryptococcal agents are known to exhibit characteristics such as cytotoxicity, high cost, and low efficacy, and many commercial agents such as fluconazole have caused drug-resistant *Cryptococcus* spp. to proliferate^[1]. The purpose of this research project is to open up the path for a new field of study within the field; testing the use of heavy-metal nanoparticles, particularly titanium dioxide nanoparticles, employed with ultraviolet-B (UVB) radiation, as an anticryptococcal agent.

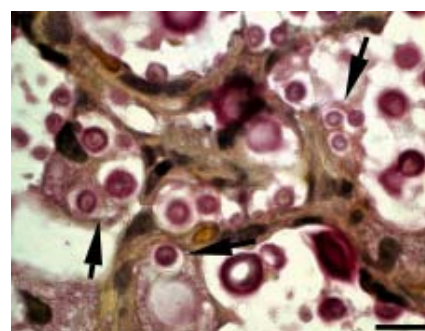


Figure 1: *Cryptococcus neoformans* fungi; the arrows point to intra- and inter-cellular alveolar blockages caused by the fungi (Figure obtained through personal correspondence with the lab of Dr. Maurizio Del Poeta).

This idea was borne out of the necessity for a low-cost antifungal agent that is simple to test, does not induce resistance in *Cryptococcus*, and is easy to build upon. TiO₂ is known, under ultraviolet-B radiation, to undergo an electrochemical reaction that triggers photocatalytic properties in the nanoparticles - it gains the ability to catalyze the hydrolysis of water to generate hydroxyl free radicals in solution. These free radicals first disrupt the cell wall, then penetrate to the cytoplasm, finally reaching the nucleus and allowing the nanoparticles to damage the DNA of bacterial and fungal cells, therefore rendering TiO₂ a promising antifungal agent^[2].

In order to confirm that the TiO₂ does not damage the macrophage cells the *Cryptococcus* infects, a toxicity test is performed. J774A.1 macrophage cells are divided into six groups; each well is exposed to either rutile TiO₂ nanoparticles, gold-citrate nanoparticles, or no nanoparticles, and is either set to be exposed to ultraviolet-B radiation for ten minutes or is not. Each well is counted after twenty-four hours of incubation following exposure. This experiment determines whether the TiO₂ nanoparticles or the radiation exhibits cytotoxicity, and whether their combination enhances cytotoxicity compared to the gold-citrate nanoparticles. After this toxicity test, a test is performed to determine the extent to which the TiO₂ nanoparticles perform as antifungal agents. The same experimental setup is performed, except the macrophage cells are exposed to *C. neoformans* initially in order to determine the effectiveness of the TiO₂ nanoparticles as antifungal agents when compared to the same nanoparticles when exposed to ultraviolet-B radiation.

Investigation into the possibility of grafting targeting molecules onto the nanoparticles is required; this method could reduce the toxicity associated with rutile nanoparticles. Further research is required to define why ultraviolet radiation impacts some nanoparticles but not others, and why some nanoparticles are useful in fighting disease. Optimization of nanoparticle concentrations and ultraviolet-B exposure is necessary if this method were to be investigated for medical purposes.

Referenced works:

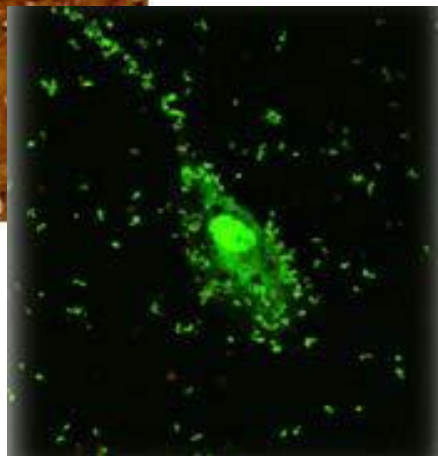
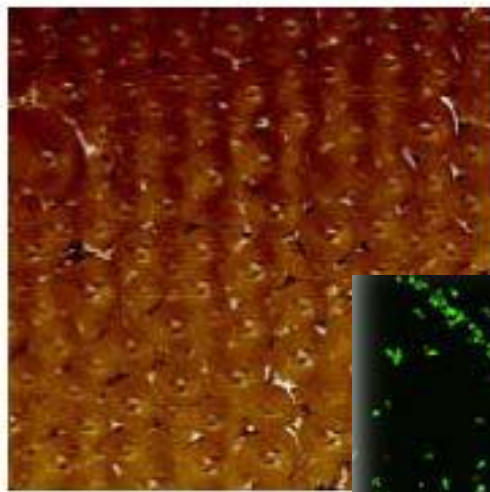
^[1] Magalhães. T.F.F. *et al.* (2013). Hydroxyaldimines as potent *in vitro* anticryptococcal agents. *Letters in Applied Microbiology*, 57, 137-143. doi: 10.1111/lam.12086

^[2] Hashimoto, K., *et al.* (2005). TiO₂ Photocatalysis: A Historical Overview and Future Prospects. *Japanese Journal of Applied Physics*, 44(12), 8269-8285. doi: 10.1143/JJAP.44.8269.

Virus/Bacteria Infection and Prevention

Chairs: Alex Lee, Purdue University; Sooditi Sood, New York University; John Jerome, Suffolk County Community College

Graduate Mentors: Yan Xu, Fan Yang



Titanium Dioxide Nanoparticles: An Effortless Path for *Staphylococcus aureus* to Infect Cells

Aaron Gochman, Sanford H. Calhoun High School, Merrick, NY

Yan Xu, Stony Brook University, Stony Brook, NY

Miriam Rafailovich, Dept. of Materials Science and Engineering, Stony Brook University, Stony Brook, NY

Steven Walker, Dept. Of Oral Biology and Pathology, Stony Brook University, Stony Brook, NY

Titanium dioxide (TiO₂) nanoparticles (NP) have been a source of recent controversy in the cosmetic industry. Found in sunscreens, toothpastes, paints, and plastics, TiO₂ is an ingredient that has deleterious effects on cells. Nanoparticles are small enough to penetrate cell membranes, a property that is not seen in most organic materials.¹ The nanoparticles destroy the cell membrane by releasing Reactive Oxygen Species (ROS).² ROS not only afflict nucleic acids, lipids, and proteins, but also have a number of adverse large-scale effects, including ulcers, stroke, and heart disease. By destroying the cell membrane, TiO₂ nanoparticles also take away the cell's main defense system. Therefore, pathogens such as bacteria have no problem infecting a cell that would otherwise be immune to infection. In this experiment, we tested *Staphylococcus aureus*, a bacterium found in the human nasal tract. The purpose of our experiment is to discern if cells exposed to these TiO₂ nanoparticles were more susceptible to bacterial infection. First, we exposed the MT3T3 skin cells and Human Fibroblasts to a 0.1 mg/mL nanoparticle concentration. A 6-well plate containing 2mg stock solution was divided so that there were control, anatase, and rutile wells. After a 24 hour incubation period, we added *Staphylococcus aureus* bacteria to control, anatase, and rutile wells. The bacteria were incubated for 90 minutes. Then, we added 1μL of BacLight® LIVE/Dead stain so that alive and dead cells could be distinguished by the color they were fluorescing. After 15 minutes, the cells were observed under the confocal microscope. The anatase and rutile wells showed a higher number of bacteria present within the cell (**Figure 1**). These results suggest that TiO₂ is an unsafe ingredient in cosmetic products because its toxicity leaves cells susceptible to bacterial infection by *Staphylococcus aureus*. Future experiments include creating a growth curve to model bacteria growth over time.

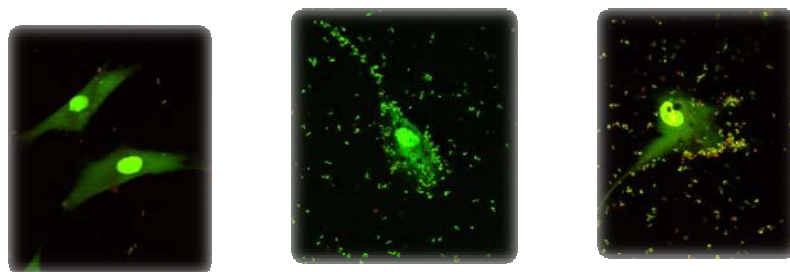


Figure 1. Control, anatase, and rutile wells, respectively, show different amounts of bacteria attacking cells. Anatase and rutile wells show greater amounts of bacteria within the cell than the control.

1. Pan, Zhi , Wilson Lee, Lenny Slutsky, Richard A. F. Clark, Nadine Pernodet, and Miriam Rafailovich. "Adverse Effects of Titanium Dioxide Nanoparticles on Human Dermal Fibroblasts and How to Protect Cells." *Small* 5.4 (2009): 511-520. *small-journal*. Web.
2. Jacobs, Johannes F., Ibo van de Poel, and Patricia Osseweijer. "Sunscreens with Titanium Dioxide (TiO₂) Nanoparticles: A Societal Experiment." *PubMed* 4.2 (2012): 103-113. *PubMedCentral*. Web.

Antibacterial Properties of Phase Separated Polymer Blends and Graphene/Graphene Oxide

Allison Lee, Hauppauge High School, Hauppauge, NY

Jing Xian Wang, Centennial High School, Ellicott City, MD

Yongyi Zhao, Newton North High School, Newton, MA

Alexander Lee, Purdue University, West Lafayette, IN

Dr. Ying Liu, Stony Brook University, Stony Brook, NY

Dr. John Jerome, Dept. of Mathematics, Suffolk County Community College, Selden, NY

Dr. Stephen Walker, Dept. of Oral Biology and Pathology, Stony Brook University, Stony Brook, NY

Dr. Miriam Rafailovich, Dept. of Material Science and Engineering, Stony Brook University, Stony Brook, NY

Currently, chemical inhibitors are one of the primary treatments against pathogenic bacteria, including but not limited to *E. coli*, *Staphylococcus Aureus*, and *Salmonella*, which can cause many diseases that often prove fatal; however, largely due to their rapid proliferation and mutation rates, bacteria are able to gain immunity to these chemical inhibitors at a relatively rapid pace¹. Mechanical destruction of the bacteria could prove to be an effective alternative that would be difficult for bacteria to adapt to. Graphene, a monolayer sheet of graphite composed of pure carbon bonded by sp² bonds², as well as the nanostructures produced by thermally induced phase separated polymer blends may provide a method for destruction of the bacterial membrane.

Mixtures of various polymers, including but not limited to PMMA, EVA, and PBr_xS, at different relative concentrations (ie. 50%/50% or 75%/25%) in toluene were spin casted onto silicon chips. The

spin casted chips with polymer solution were then annealed in a vacuum oven at 170⁰C, allowing the

polymers to phase separate, a process in which polymers that do not mix into a uniform solution distribute to form microstructures that may rupture the bacterial lipid membrane. Since spin casting of graphene solution deposited tiny graphene clusters that proved too small to produce significant results on bacteria, the silicon chips were instead dipped into graphene and graphene oxide (GO) suspended in solution, depositing significantly larger clusters of graphene and GO onto the silicon chips. Bacteria in medium were pipetted onto the silicon chips and the effects on the bacteria mortality attached to the surface were observed under the confocal microscope using a live/dead stain.

Atomic Force Microscope and optical microscope images (Figure 1) confirm that polymers were properly phase separated. Though spin casting graphene did not produce significant bactericidal results, the method of dipping the silicon chips killed bacteria around the graphene.

In the future, we hope to improve the microstructures produced by the phase separated polymer blends for optimal puncturing of the bacteria, which can be done by altering the relative concentrations of the polymers, adjusting annealing time and temperature, and using new combinations of polymers and solution. Graphene has been shown to potentially destroy the bacterial membrane by extraction of the phospholipid membrane³; we therefore hope to explore methods to demonstrate or disprove this, possibly utilizing the scanning electron microscope (SEM).

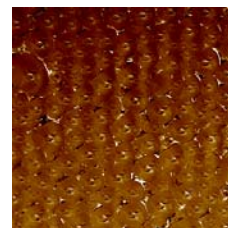


Figure 1 : AFM image of phase separated polymer blend of EVA and PBr_xS

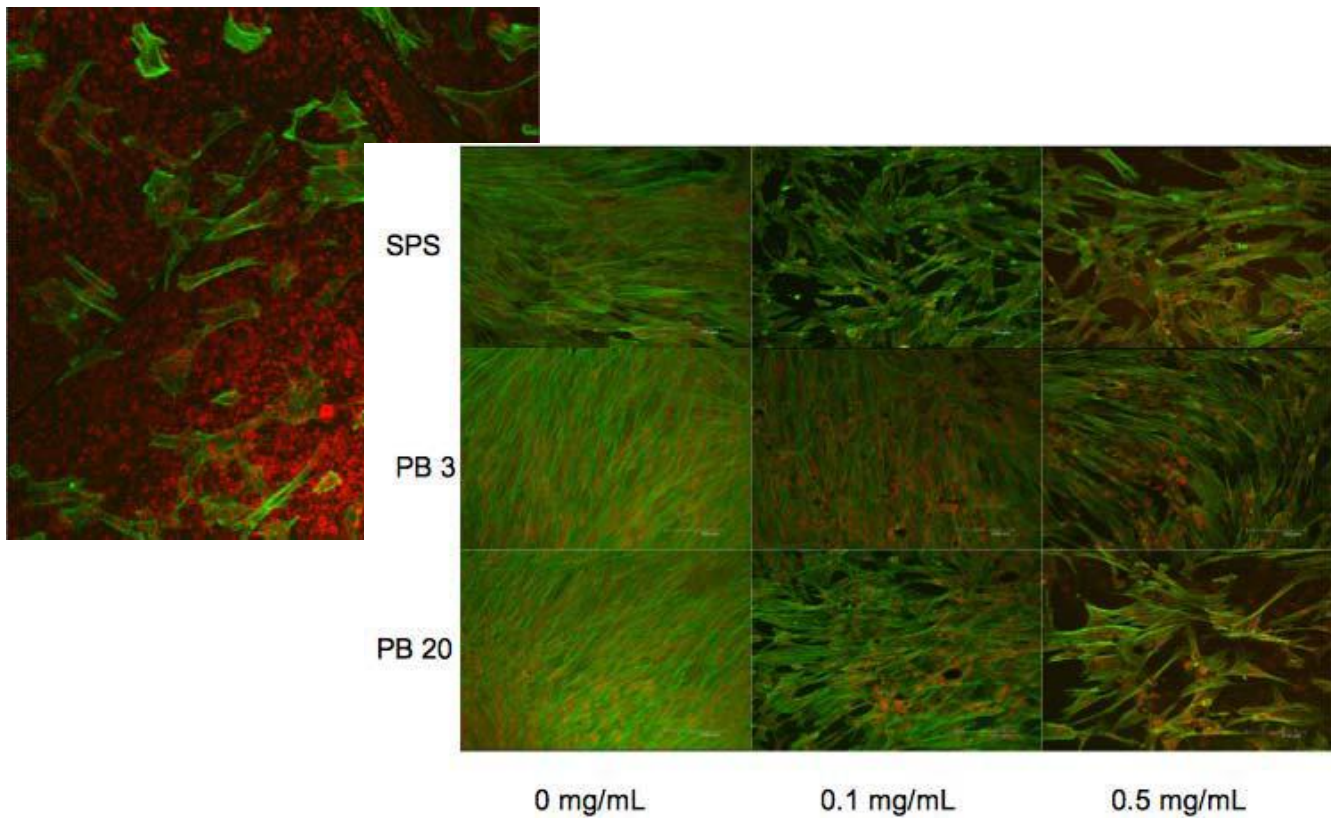
¹ Perez F, Hujer AM, Hujer KM, Decker BK, Rather PN, Bonomo RA (2007) Global challenge of multidrug-resistant *Acinetobacter baumannii*. *Antimicrob Agents Chemother* 51:3471–3484

² Geim, A. K.; Novoselov, K. S. The Rise of Graphene. *Nat. Mater.* **2007**, *6*, 183–191.

³ Tu, Y, et. al. "Selective bactericidal activity of nanopatterned superhydrophobic cicada *Psaltoda claripennis* wing surfaces." *Nature Nanotechnology* 8 (2013): 594-601. *Nature Nanotechnology*. Web. 12 July 2013.

Dental Pulp Stem Cells

Chairs and Graduate Mentors: Yingjie Yu, Stony Brook University; Luidi Zhang, Jane Zhang, Stony Brook University



The Effects of Electrically Conductive Surfaces, Such as Poly(3-hexylthiophene), on Dental Pulp Stem Cell Differentiation

Abraham Gross, Rambam Mesivta Highschool, Lawrence, NY

Evelyn Abramov-Kandov, Yeshiva University High School for Girls, Holliswood, NY

³Jianyuan Zhang, Department of Material Science and Engineering

³Chung-Chueh Chang, Advanced Energy Research and Technology Center (AERTC)

³Yingjie Yu, Department of Material Science and Engineering

³Marcia Simon, Department of Oral Biology and Pathology

³Miriam Rafailovich, Department of Materials Science and Engineering

³Stony Brook University, Stony Brook, NY

Uncovering means of inducing reliable stem cell differentiation is currently an important area of research, with conventional methods including the use of chemical stimulation¹. Research has shown that electrical stimulation can also generate differentiation in certain stem cell groups². Poly(3-hexylthiophene) or P3HT, an organic photovoltaic polymer, has been shown to stimulate neuronal cells via electrical signaling and generate responses without harming the cells and their ability to proliferate³. The purpose of the project was to determine P3HT's effects on dental pulp stem cell (DPSC) differentiation as an alternative to chemically-induced DPSC differentiation.

Before an experiment on P3HT's effects of DPSC differentiation could be performed, the morphological and photoreactive traits of the polymer had to be determined, and possible cytotoxicity monitored. 5.08mg/mL and 14.8 mg/mL P3HT/chlorobenzene solutions were prepared and spin-coated onto silicon (Si) wafers and glass slips, with one (Si) sample of each concentration placed in media for a 72 hour period. Four (Si) wafers were examined by an Atomic Force Microscope (AFM) to compare their morphology using one 'dry' analysis and one 'wet' analysis, and 2 glass slips were analyzed using UV-VIS to determine the absorption spectra of each P3HT concentration. Additionally, 12 P3HT-coated (Si) wafers were plated with approximately 10,000 DPSC each and left in an incubator, to be removed for preservation on days 3, 5, and 8 and stained with Alexa flour 488 and PI dyes, which makes actin appear green and nuclei red, in order to count cells under a Confocal Microscope to establish a growth curve and analyze proliferation.

AFM results showed that in both the 'wet' and 'dry' samples, the 14.8 mg/mL sample showed greater variance in morphology over the 5.08mg/mL sample. UV-VIS determined that the 14.8mg/mL absorbed more effectively than the 5.08mg/mL, and absorbed most in both samples at the wavelengths between approximately 650 to 420. Using Confocal Microscopy, it appeared the amount of DPSC on both samples decreased from the starting number and then showed minor proliferation, indicating possible cytotoxicity [Fig 1].

Due to the absorption spectra of P3HT which causes a red appearance, the nuclei were masked, making it difficult to accurately count cells and therefore indicate the effects of the polymer on DPSC proliferation [Fig 1]. In order to do so, a second growth experiment is to be carried out using P3HT on a glass platform rather than (Si) in order to observe living cells underneath a light microscope to better understand the possible cytotoxicity of P3HT. Additionally, PEDOT:PSS, another electrically conductive surface, is also being investigated as a possible alternative to P3HT.

¹Királya, M., Porcsalmya, B., Patakib, A., Kádára, K., Jelitaic, M., Molnára, B., Hermann, P., Gerae, I., Grimm, W.D., Ganssg, B., Zsemberyb, A., and Varga, G. (October 2009). Simultaneous PKC and cAMP activation induces differentiation of human dental pulp stem cells into functionally active neurons. *Neurochemistry International*, Volume 55, Issue 5, Pages 323–332.

²Sauer, H., Rahimi, G., Hescheler, J., and Wartenberg, M. (1999). Effects of electrical fields on cardiomyocyte differentiation of embryonic stem cells. *Journal of Cellular Biochemistry*, 75:710–723.

³Ghezzi, D., Antognazza, M.R., Maschio, M.D., Lanzarini, E., Benfenati, F., and Lanzani, G. (2011, January 25). A hybrid bioorganic interface for neuronal photoactivation. *Nature Communications*, article number 166.

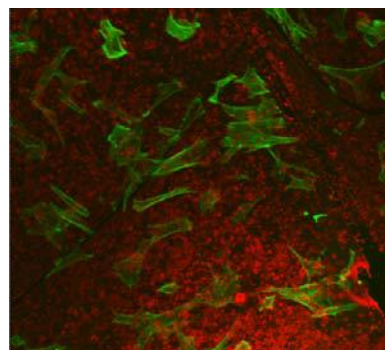


[Fig 1] Stained DPSC under Confocal Microscope, day 8, 5.08mg/mL (scale bar shown to be 149.52 μ m)

The effect of TiO₂ concentration on dental pulp stem cells using SPS and PB substrates

Min Seong Kim (Jericho High School, NY), **Alec Silverstein** (Biotechnology High School, NJ), **Chung-Chueh Chang, Jianyuan Zhang, Miriam Rafailovich** (Dept. of Materials Sciences, Stony Brook University NY), **Marcia Simon** (Dept. of Oral Biology and Pathology, Stony Brook University, NY)

Dental pulp stem cells, as stem cells with differentiation and proliferation capability, repair root canals and can be found in tooth cavities; these properties make them essential for use in regenerative endodontics and similar fields. During the healing process for tooth decay, dental pulp stem cells may frequently interact with titanium dioxide [TiO₂] nanoparticles; TiO₂ is found in many common consumer items such as toothpaste due to its use as a bleaching agent (Johnston et. al., 2009). TiO₂ has previously shown to be toxic via oxidative stress (Meena et. al., 2012). Different substrate environments were used, including sulfonated polystyrene [SPS] and polybutadiene [PB] to see the cytotoxic effect of TiO₂ in varying conditions. The purpose of this research project was to test different concentrations of TiO₂ nanoparticles and various polymer thin-film substrates to determine the effect of each factor individually, as well as the combined effect of nanoparticles and polymers in the environment as a whole on stem cell proliferation, or growth, and differentiation, or formation of different types of body cells.

The different solutions made for spin casting included 3 mg/mL, 20 mg/mL PB, and 7 mg/mL SPS. Spin-casting was performed with a photoresist spin-casting machine to make different thin-film substrates. Standard plating procedure was used, with trypsin used to detach cells from flasks and MEM alpha [1X] as the cellular media. Counting procedure involved using a hemocytometer to extrapolate the total amount of cells in each sample. Lastly, confocal microscopy obtained pictures of the three different polymers, each with the three different TiO₂ concentrations [0 mg/mL, 0.1 mg/mL, and 0.5 mg/mL], after fixing the samples to kill the cells and staining the samples to observe cell structure and growth patterns.

The results of the experiment supported a trend of decreasing cell growth with increasing TiO₂ concentration. In addition, when comparing the different polymer films, it seemed that PB films were better for cell growth than SPS, and thinner films were also more effective [PB 3 over PB 20]. The confocal images taken of the cells with dye identifying cell structure and proliferation also supported these conclusions [Figure 1].

Due to the decreased cell density induced by TiO₂ nanoparticles, TiO₂ seems to be toxic to cell growth with increasing concentration, or dose. In addition, nanoparticle toxicity has also been shown to be a function of the polymer substrate. In the future, experiments will be conducted to observe the relationship between TiO₂, substrate composition, and differentiation of dental pulp stem cells.

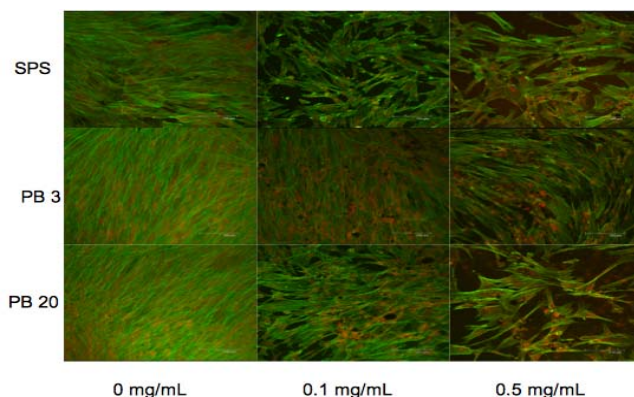


Figure 1: Confocal Images of Dental Pulp Stem Cell Growth in Different Environments

References

- Johnston, H. J., Hutchinson, G. R., Christensen, F. M., Peters, S., Hankin, S., & Stone, V. (2009). Identification of the mechanisms that drive the toxicity of TiO₂ particulates: the contribution of physicochemical characteristics. *Particle and Fibre Toxicology*, 6(33). <http://dx.doi.org/10.1186/1743-8977-6-33>
- Meena, R., Rani, M., & Pal, R. (2012). Nano-TiO₂-induced apoptosis by oxidative stress-mediated DNA damage and activation of p53 in human embryonic kidney cells. *Applied Biochemistry and Biotechnology*, 167, 791-808.

Developing an Alternative Root Canal Filler to Stimulate Dental Pulp Stem Cell Proliferation and Differentiation

Ruiyi Gao, Lincoln Sudbury Regional High School, Sudbury, MA

Amanda Shi, Westlake High School, Westlake Village, CA

Liudi Zhang, Stony Brook University, Stony Brook, NY

Miriam Rafailovich, Dept. of Material Science and Engineering, Stony Brook University, NY

Marcia Simon, School of Dental Medicine, Stony Brook University, NY

Gutta-percha, an endodontic material, has been the primary root canal filling substance used in dental care and therapy since the late nineteenth century. However, cytotoxicity studies have shown that gutta-percha, due to its high concentration of zinc oxide^[1], can hinder dental pulp stem cell (DPSC) proliferation^[2]. Hence, the purpose of this project is to engineer an alternative root canal filler by combining polyisoprene (PI), a primary constituent of gutta-percha, with different additives in varying concentrations to identify the optimal blend for improved DPSC proliferation and differentiation.

In order to study and compare the effects of different combinations of PI and additives on the proliferation and differentiation of DPSCs, solutions of 15 and 20 mg/mL of PI mixed with 0.1 and 0.5 mg/mL titanium dioxide (TiO₂) nanoparticles (rutile and anatase) as well as 0.5, 5 and 10 mg/mL ProRoot Mineral Trioxide Aggregate (MTA) were prepared and spun onto [100] oriented silicon wafers to create samples. 15 mg/mL PI was chosen as the base polymer of the root canal filler after ellipsometry tests. Optical microscopy was then used to analyze the surface morphology of the samples in both dry and wet conditions. DPSCs were then plated onto the samples in a 24 well dish with 10,000 cells per well for an 8-day growth curve and a 28 day differentiation experiment. Cells were counted using a hemocytometer and plotted into a growth curve by cell density. The day 8 cells were then fixed with formalin and stained with Alexa Fluor 488 dye and Propidium Iodide dye to stain the actin fibers and nucleus respectively. The fixed and stained cells were then imaged under the confocal microscope for further analysis.

Results of cell counting and trends demonstrated by the 8 day growth curve indicate that of the PI combinations involving TiO₂, 0.5 mg/mL stimulates the most cell growth. Confocal imaging further

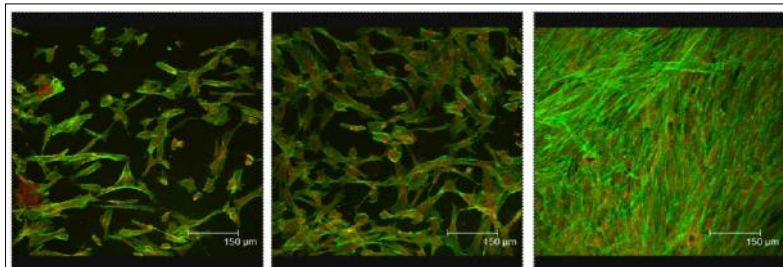


Figure 1. Confocal images of day 8 DPSCs (left, pure PI; middle, PI combined with 0.1 mg/mL anatase; right, PI combined with 0.5 mg/mL anatase).

verified the results of cell counting, with 0.5 mg/mL TiO₂ (anatase and rutile) having the highest confluence and pure PI having the lowest (Fig. 1). The cell counting results and trends of the 8 day growth curve of the PI combinations involving ProRoot MTA also induced a greater DPSC proliferation rate at the concentration of 5 mg/mL ProRoot MTA.

Future work will consist of investigating the effects of dexamethasone, a steroid that can stimulate differentiation, on DPSCs plated for 28 days on silicon wafers spun-cast with 15 mg/mL PI and varying additives (0.5 mg/mL titanium dioxide [rutile and anatase] and 5 mg/mL ProRoot MTA). The atomic force microscope will also be used to analyze the surface morphology of each sample, and differentiate between their structural characteristics.

¹ Pascon, Elizeu A., and Larz S. W. Spangberg. (1990, September). "In Vitro Cytotoxicity of Root Canal Filling Materials: 1. Gutta-percha." *Journal of Endodontics*, 16.9, 429-133

² Zhang, Liudi. "Interaction of Commercially Gutta Percha Substrates with Mouse Osteoblasts and Dental Pulp Stem Cells." Powerpoint presentation. Stonybrook University, Stonybrook, NY.

Featured Garcia Program Guest Lectures

June 24:

“Tattoo removal and bio-degradable inks” **Joe Miccio**, Graduate Student, Stony Brook University, Stony Brook, NY

“Techniques and challenges in endodontics” **Chris Joubert**, DDS, Dental School, Stony Brook University, Stony Brook, NY



June 25:

“The biology of blood” **Dennis Galanakis**, MD, Stony Brook Medical Center, Stony Brook, NY

“Dental Pulp Stem Cells” **Marcia Simon**, PhD, Stony Brook University, Stony Brook, NY

“Alternative fuel sources” **Devinder Mahajan**, PhD, Stony Brook University, Stony Brook, NY

“Flame retardant nanocomposites” **Harry He and Kai Yang**, Graduate Students, Stony Brook University, Stony Brook, NY

“Electrospinning polymers” **Ying Liu**, PhD, Stony Brook University, Stony Brook, NY

June 27:

“Challenges in wound healing research” **Richard Clark**, MD, Stony Brook University, Stony Brook, NY

“Introducing the Advanced Energy Research Center and 3D printers” **Jim Smith**,
Advanced Energy Research Center, Stony Brook University, Stony Brook, NY

June 28:

“Theory of rheology” **Steven Schwarz**, PhD, Queens College, Flushing, NY

July 1:

“Patents and intellectual property” **Donna Tummaniello**, PhD, Stony Brook
University, Stony Brook, NY

July 2:

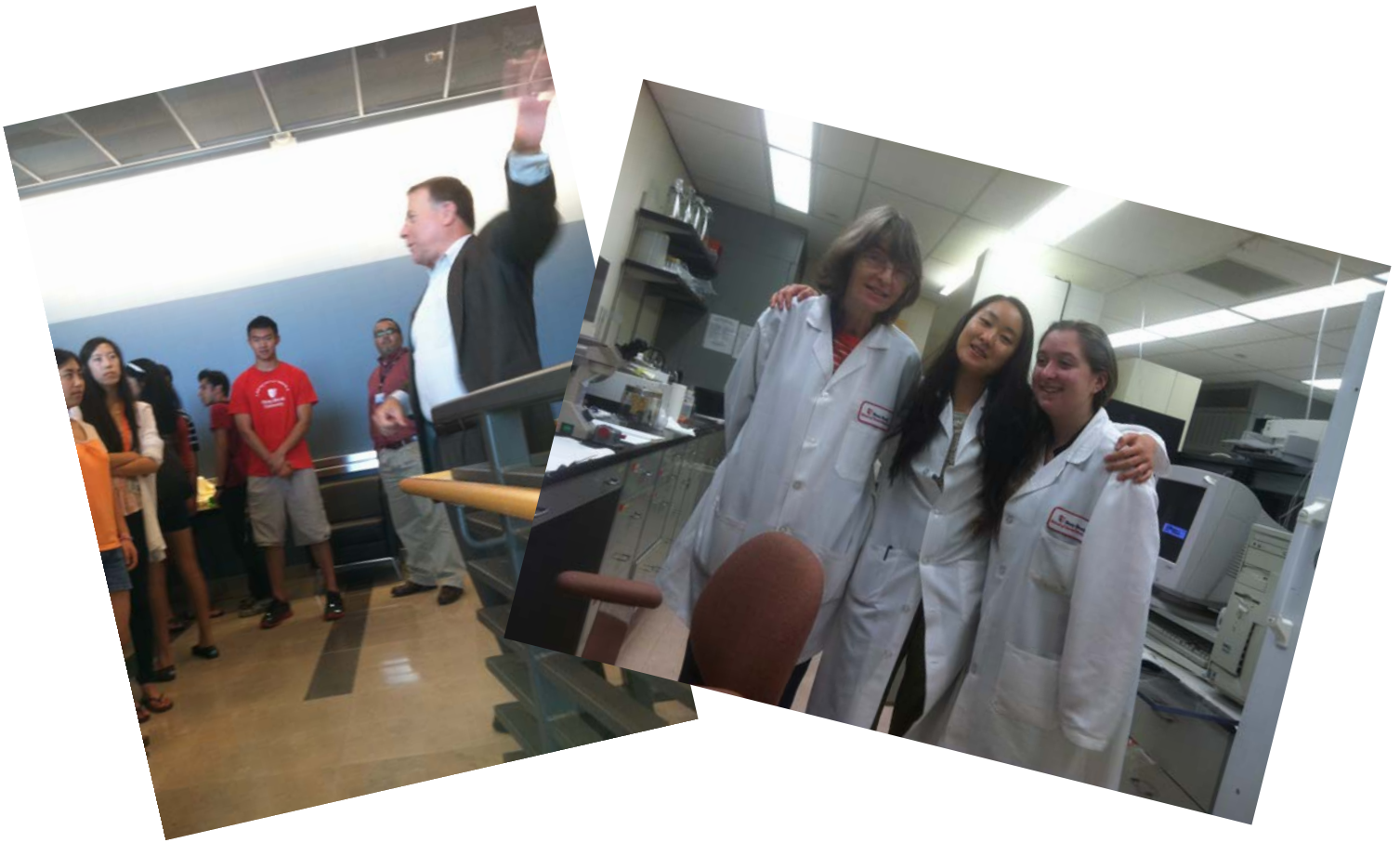
“Introduction to microbiology” **Mauritzio Del Poeta**, PhD, Stony Brook University,
Stony Brook, NY

“Bioethics and stem cell research” **Brook Ellison**, PhD, Director of Bioethics, Stem
Cell Research Center, Stony Brook University, Stony Brook, NY

“Molecular modeling of nanocomposites” **Dilip Gersappe**, PhD, Stony Brook
University, Stony Brook, NY

July 3:

“Nanotoxicology” **Tatsiana Mironava**, PhD, Stony Brook University, Stony Brook, NY





Donate food
here.
Pickup on
Thursday.

One more way to feed the hungry on Long Island ans show that Garcia students care:

Students of Garcia contributed over \$600 in food from unused meal cards at the end of the summer to Island Harvest.

The Garcia Program gratefully acknowledges support from the Louis Morin Charitable Trust .